Biogeosciences Discuss., 7, 4341–4384, 2010
www.biogeosciences-discuss.net/7/4341/2010/
doi:10.5194/bgd-7-4341-2010

Biogeosciences
Discussions

Crustal uplifting rate associated with late-Holocene glacial-isostatic rebound at Skallen and Skarvsnes, Lützow-Holm Bay, East Antarctica: evidence of a synchrony in sedimentary and biological facies on geological setting

Y. Takano[1], Y. Yokoyama[1,2], J. J. Tyler[1,2,3,*], H. Kojima[4], M. Fukui[4], T. Sato[5], N. O. Ogawa[1], N. Suzuki[6], H. Kitazato[1], and N. Ohkouchi[1,3, 7]

[1]Institute of Biogeosciences, Japan Agency for Marine-Earth Science and Technology (JAMSTEC), 2-15 Natsushima, Yokosuka, 237-0061, Japan
[2]Ocean Research Institute, University of Tokyo, 1-15-1 Minami-dai, Tokyo, 164-8639, Japan
[3]Department of Earth and Planetary Sciences, University of Tokyo, 7-3-1 Hongo, Tokyo, 113-0033, Japan

[4]The Institute of Low Temperature Science, Hokkaido University, N19 W8,
Kita-ku, Sapporo, 060-0819, Japan
[5]Faculty of Integrated Arts and Sciences, Hiroshima University, Kagamiyama,
Higashi-Hiroshima, 739-8521, Japan
[6]Department of Natural History Sciences, Faculty of Science, Hokkaido University, N10 W8,
Kita-ku, Sapporo, 060-0810, Japan
[7]Department of Environmental Science and Technology, Tokyo Institute of Technology,
4259 Nagatsuda, Midori-ku, Yokohama, Kanagawa, 226-8502, Japan
[*]now at: Department Earth Sciences, Oxford University, Oxford, OX1 3PR, UK

Received: 20 April 2010 – Accepted: 28 May 2010 – Published: 8 June 2010

Correspondence to: Y. Takano (takano@jamstec.go.jp)

Published by Copernicus Publications on behalf of the European Geosciences Union.

Abstract

We determined the mean crustal uplifting rate during the late Holocene along the Soya Coast, Lützow-Holm Bay, East Antarctica, by dating a marine-lacustrine transition recorded in lake sediments. We focused on temporal variations in the chemical composition of sediments recovered from Lake Skallen Oike at Skallen and Lake Oyako at Skarvsnes. Both sets of lake sediments record environmental changes associated with a transition from marine to lacustrine (fresh water) settings, as indicated by analyses of sedimentary facies for carbon and nitrogen contents, nitrogen isotopic compositions ($^{15}N/^{14}N$), and major element concentrations. Changes in the dominant primary producers during the marine-lacustrine transition were also clearly revealed by biogenic Opal-A, diatom assemblages, and gradient gel electrophoresis (DGGE) with 16S rRNA gene analysis. Geochronology based on radiocarbon dating of acid-insoluble organic carbon suggested that the environmental transition from saline to fresh water occurred at 2940±100 cal yr BP at L. Skallen and 1060±90 cal yr BP at L. Oyako. Based on these data and a linear approximation model, we estimated a mean crustal uplifting rate of 3.6 mm yr^{-1} for the period since the marine-lacustrine transition via brackish condition; this uplift is attributed to glacial-isostatic rebound along the Soya Coast. The geological setting was the primary factor in controlling the emergence event and the occurrence of simultaneous changes in sedimentary and biological facies along the zone of crustal uplift.

1 Introduction

Previous studies have modeled glacial rebound and sea-level change arising from the recession of large-scale continental ice sheets since the Last Glacial Maximum (LGM), which led to eustatic sea-level changes and glacio-isostatic responses in Antarctica (e.g. Nakada and Lambeck, 1989; Lambeck, 1993; James and Ivins, 1998; Bentley, 1999; Yokoyama et al., 2001; Anderson et al., 2002; Huybrechts, 2002; Ivins and James, 2005; Yokoyama et al., 2006). Since the initial work of Yoshikawa and Toya (1957), studies undertaken in the Lützow-Holm Bay area of East Antarctica have advanced our knowledge of relative sea-level change during the Holocene. Geological approaches involving techniques such as bedrock GPS and VLBI (Very Long Baseline Interferometry) measurements (e.g. Yoshida and Moriwaki, 1979; Hayashi and Yoshida, 1994; Igarashi et al., 1995; Kaminuma et al., 1996; Maemoku et al., 1997; Miura et al., 1998a, b, c; Soudarin et al., 1999; Shibuya et al., 2003; Fukuzaki et al., 2005; Ohzono et al., 2006). Maemoku et al. (1997) suggested that the East Antarctic Ice Sheet (EAIS) covered the southern part of Lützow-Holm Bay during the LGM. The Holocene marine limit along the Soya Coast is estimated to have been approximately 18 m above mean sea level (a.m.s.l.), based on analyses of indigenous raised beach deposits such as bivalve fossils (*Laternula elliptica*: Miura et al., 1998c) combined with modeling studies (Nakada et al., 2000), which indicate considerable regional isostatic rebound in response to a reduction in ice volume. Based on these studies, it was concluded that most of the present-day ice-free areas along the southern Soya Coast had become free of the EAIS by the mid-Holocene (Miura et al., 1998c). As an endemic suspension feeder, radiocarbon dating of fossil *L. elliptica* tests is a potentially valuable means of assessing past relative sea-level changes. However, such applications are potentially limited by our understanding of the ecological characteristics of *L. elliptica*, thus requiring further consideration of the significance of these fossil dates.

The advances made in the above studies have led to the development of plausible models of crustal movement within coastal areas in East Antarctica. Although little is known of the geology of the Soya Coast within Lützow-Holm Bay, sedimentary facies exposed in ice-free coastal areas provide important clues in reconstructing the paleo-environment (e.g. Matsumoto et al., 2006). In this study, we focus on temporal variations in the chemical and microbiological assemblages of sediments recovered from two lakes (at Skallen and Skarvsnes) along the Soya Coast, Lützow-Holm Bay. We identified marine-lacustrine transitions recorded in the lake sediments with the aim of accurately determining the timing of emergence. Our data are combined with previously published raised beached dates using *L. elliptica*, thereby enabling the development of a quantitative approximation model of the mean crustal uplifting rate during the late Holocene.

2 Materials and method

2.1 Geological location and sampling

Imura et al. (2003) and co-workers documented the spatial distribution of lakes upon the continental ice margin of the Soya Coast region, revealing a wide variety of profiles ranging from freshwater lakes affected by continental glaciers to saline lakes that evaporated following their isolation from the ocean in response to Holocene uplift. Skallen is a 14.1 km^2 ice-free coastal area of rocky hills located in east Lützow-Holm Bay (Fig. 1). Figure 2 shows photographs of the landscape in this area and of the water inlet and outlet at Lake Skallen Oike (hereafter L. Skallen; see Table 1), which is located in central Skallen. Skarvsnes is the largest ice-free area (61 km^2) along the Soya Coast. Lake Oyako (hereafter L. Oyako) is located within Skarvsnes, near Kizahashi Beach (Miura et al., 1998c). These two lakes are presently separated from the open ocean by sills with heights (overflowing points) of 10 and 5 m a.m.s.l., respectively. The present tidal range along Soya coast is within ca. ±0.5 m (e.g. Aoki et al., 2000). Lake sediments were collected from these lakes using push-type corers during the 47th Japan Antarctica Research Expedition (December 2005 to February 2006; see the core images in Fig. 3). The cores were cut into 3–10 cm intervals and stored at 0–4 °C or –20 °C for onshore geochemical analysis and 16S rRNA analysis, respectively.

2.2 Geochemical analysis of sedimentary facies

Major elements (MgO, Al_2O_3, SiO_2, K_2O, CaO, TiO_2, MnO, and Fe_2O_3) were analyzed by X-ray fluorescence (JSX-3211, JEOL), calibrated using Geological Survey of Japan (GSJ) standard materials (JA-1, JA-3, JB-1a, JB-3, JG-2, JG-3, JGb-1, JP-1, JLK-1, JLs-1, JDo-1, JSl-1, JCh-1, JR-3, JMn-1, JSd-2, and JSd-3) (e.g. Imai et al., 1995; 1996; 1999). The presented data represent the average value of two analyses. Opal-A was identified by X-ray diffraction (XRD, Mac Science Co. Ltd.) to acquire the signal of amorphous biogenic silica derived from diatoms, namely siliceous primary producers. Color data were obtained using a digital color meter (SPAD 503, Konica Minolta) and revised Standard Soil Color Charts (e.g. Oyama and Takehara, 2005).

After HCl pretreatment for freeze-dried sediments, carbon and nitrogen isotopic ratios were mainly determined using an isotope ratio mass spectrometer (IRMS; Delta Plus XP, ThermoFinnigan) coupled with a Flash elemental analyzer (EA; EA1112, ThermoFinnigan) via a Conflo III interface (e.g. Ohkouchi et al., 2005). For a small number of analyses we also used an elemental analyzer-isotope ratio mass spectrometer (Costech 4010 Elemental Analyzer; ThermoFinnigan Delta plus Mass Spectrometer). Carbon and nitrogen isotopic compositions are expressed as the per mil (‰) deviation from the standard, as follows: $\delta^{13}C=[(^{13}C/^{12}C)_{sample}/(^{13}C/^{12}C)_{standard}-1]\times1000$ (‰) for carbon and $\delta^{15}N=[(^{15}N/^{14}N)_{sample}/(^{15}N/^{14}N)_{standard}-1]\times1000$ (‰) for nitrogen. Elemental analyses of carbon, nitrogen, and sulfur were performed using a Micro CORDER JM10 (J-Science Lab Co., Ltd.). Some of the sedimentary organic carbon fractions after HCl pretreatment were analyzed to obtain radiocarbon age (^{14}C), corrected after the $\delta^{13}C$ value, using an accelerator mass spectrometer (AMS) housed at the University of Tokyo, Japan (Yokoyama et al., 2007), and by Beta Analytic Inc., Florida, USA.

In order to refine our uplift model, we re-assessed previously published radiocarbon ages of fossil *L. elliptica* shells sampled from raised beaches. In particular, we reconsidered the depth habitat, based on a review of ecological literature, in order to more accurately determine the age of sedimentation of these fossils.

2.3 Diatom analysis to confirm biological facies

In addition to chemical analysis for amorphous biogenic silica, sediments from core Sk5S were prepared for diatom analysis following a standard procedure, involving heating (70 6∘C) in hydrogen peroxide to remove organic matter, followed by the addition of 10% HCl to remove carbonates (Battarbee et al., 2001). Following chemical treatment, samples were rinsed three times in de-ionized water and concentrated by centrifugation (1500 rpm). The residual diatom material was mounted upon microscope slides using Norland® optical adhesive, and fixed under ultraviolet light. A minimum of 300 diatoms were counted per sample using phase-contrast light microscopy at 400× and 1200× (oil immersion) magnification, following Hirano (1983), Krammer and Lange-Bertalot (1986, 1988, 1991a, b), Medlin and Priddle (1990), and Spaulding et al. (2008).

2.4 DGGE analysis with 16S rRNA gene

DNA-based analyses were conducted on the samples of 12 sections (0–10, 50–60, 100–110, 150–160, 160–170, 170–180, 180–190, 190–200, 240–250, 290–300, 320–330, and 350–360 cm). Total DNA was extracted from 0.5–1.0 g of each sample using UltraClean Soil DNA Isolation Kit (Mobio, Carlsbad, CA, USA).

For denaturing gradient gel electrophoresis (DGGE) analysis, fragments of 16S rRNA gene were amplified by polymerase chain reaction (PCR) using primers GC341f and 907r (Muyzer et al., 1996). The PCR amplification was initiated with denaturation step of 2 min at 94 °C, followed by 30 cycles of 94 °C for 30 s, 45 °C for 30 s, 72 °C for 45 s. A final extension was performed for 10 min at 72 °C. The PCR products were subjected to DGGE analysis with a 1.5-mm-thick 6% (w/v) polyacrylamide gel (acrylamide:bisacrylamide = 37.5:1), using a DCode system (Bio-Rad, Hercules, CA, USA). The range of denaturant gradient was 20% to 60% (100% corresponds to 40% – v/v – formamide and 7 M urea). The electrophoresis was run in 0.5× TAE buffer (20 mM Tris, 10 mM acetic acid, and 0.5 mM EDTA, pH 8), at 60 °C for 16 h at a constant voltage of 100 V. After the electrophoresis, the gels were stained with SYBR green I for 45 min, and then photographed with a UV transillumination. Several major bands were cut from the gel, and DNA fragments in the pieces of gel were eluted by incubation in 10 µl of sterile water overnight at 4 °C. From 1 µl of each resulting solution, DNA fragments were re-amplified by PCR and then subjected to sequencing. Prior to the sequencing, each PCR product was purified with ExoSAP-IT (USB Corporation, Cleveland, OH, USA). Sequencing reactions were performed with the BigDye Terminator v3.1 Cycle Sequencing Kit (Applied Biosystems, CA, USA) and the products were analyzed using an ABI PRISM 3100-Avant Genetic Analyzer (Applied Biosystems, CA, USA). The sequences obtained were compared to those in the DDBJ/EMBL/GenBank database by using the online BLAST program located at the NCBI website (http://www.ncbi.nlm.nih.gov/).

3 Results

3.1 Geochemistry and nitrogen isotopic compositions of sedimentary facies

In the core sediments, we observed distinct soft-mat laminations made up of microbial mat, silt and clay layers, unaffected by bioturbation (Fig. 3). The upper sections of core Sk5S (from L. Skallen) consist of soft dark-black microbial mat with olive black, greenish black, and bluish black coloring, while the lower sections of the core are largely gray to dark gray (Fig. 3a and c). Although the reason is unconfirmed, a sediment deformation was observed at the depth of 260 cm in L. Skallen, likewise 110 cm in Ok5S (see also Fig. 4). Since we could not distinguish the sedimentary facies by the sediment color monitoring and lithological description, we conducted geochemical analysis including major element and nitrogen isotopic composition.

Figure 4 shows depth profiles of chemical trends in the two cores. Lake sediments within cores Sk5S (L. Skallen) and Ok5S (L. Oyako) record a transition from marine to lacustrine conditions including temporal brackish conditions, as indicated by various

Title Page
Abstract Introduction
Conclusions References
Tables Figures
|◀ ▶|
◀ ▶
Back Close
Full Screen / Esc
Printer-friendly Version
Interactive Discussion

chemical components such as carbon and nitrogen contents, nitrogen isotopic compositions, and major element contents (Fig. 4). The total carbon (TC) content shows a marked increase beginning at 180 cm depth in core Sk5S and 90 cm depth in Ok5S. In Sk5S, the sedimentary TC content is less than 4 wt% in sediments deeper than 180 cm, but is up to 7.9 wt% immediately above 180 cm and 19.7 wt% at 45 cm depth. Although the trend is less clear in Ok5S, the TC content jumps from 2.5 to 6.4 wt% passing upward across 90 cm depth. Similar trends are observed in both cores in profiles of total nitrogen (TN) and C/N. In Sk5S, total sulfur (TS) content is strongly elevated at 80–180 cm depth, probably reflecting the accumulation of sulfides under meromictic conditions. The nitrogen isotopic composition ($\delta^{15}N$) of bulk organic matter within lake sediments shows a significant shift at the marine-lacustrine transition. Representative values of +6.1‰ at the mid-depth of 315.0 cm in Sk5S and +6.7‰ at the mid-depth of 151.5 cm in Ok5S are indicative of marine sediments (Fig. 4), whereas the ^{15}N-depleted isotopic composition of shallow sediments within the cores (~0‰) suggests that nitrogen assimilation occurred in a freshwater environment.

3.2 Major components of sedimentary facies and opal-A signatures in marine stage

The compositional trends of inorganic major elements also indicate a marked marine-lacustrine transition in each of the cores (Fig. 4). The lower, marine sediments in both lake cores were substantially SiO_2-enriched (<73% in Sk5S; <57% in Ok5S) indicating high SiO_2 end-member values for the marine sediments and low SiO_2 associated with more recent freshwater conditions. The mixture of these two end-members can be illustrated in a SiO_2-Al_2O_3 diagram, in which contrasting mixing trends are observed across 180 cm depth in core Sk5S and 90 cm depth in core Ok5S (Fig. 5). In both cores, the high SiO_2 end-member compositions suggest a large contribution by biogenic silica in Antarctic seawater (Cortese et al., 2004) and in turn indicating an abundance of diatoms (Figs. 5 and 6). X-ray diffraction analyses of sediment from core Sk5S indicate abundant opal-amorphous (opal-A) in deeper parts of the section (355 cm) relative to that in shallower parts (165 cm), supporting the biological origin of this silicate (Fig. 6). The reduction in opal-A abundance within the shallower part of the section suggests a decrease in diatom abundance, possibly associated with a net reduction in productivity, an increase in non-silicate photoautotrophs such as cyanobacteria (unpublished data) and an increase in dilution by minerogenic matter. It is interesting to note that Fe_2O_3 (wt%) in the Sk5S sediment was negatively correlated with SiO_2(wt%) and positively correlated with total C&N contents. Based on the Fe_2O_3-Al_2O_3 plot, the main deposition source of iron oxide in L. Skallen might have changed during the marine-lacustrine transition, while L. Oyako has followed a constant trend. Bed-rock is one of possible sources of iron oxide imported from seeping ground water/surface water and wide catchment basin in the Lützow-Holm Bay region (e.g. Kawakami and Motoyoshi, 2004; see also Fig. 2). X-ray diffraction analyses of sediment from core Sk5S indicate abundant opal-amorphous (opal-A) in deeper parts of the section (355 cm) relative to that in shallower parts (165 cm), confirming the biological origin of silicate (Fig. 6). The reduction in opal-A abundance within the shallower part of the section suggests a decrease in diatom abundance and an increase in non-silicate photoautotrophs such as cyanobacteria (unpublished data).

3.3 Radiocarbon age determination of sedimentary organic matter

The geochemical data indicate that environmental change (i.e., a marine-lacustrine transition) associated with disconnection of the lakes from marine conditions occurred at 180 cm depth in core Sk5S (L. Skallen) and 90 cm depth in Ok5S (L. Oyako). We obtained AMS radiocarbon dates for organic matter in the cored sediments both above and below these depths (Fig. 4 and Table 2). Yoshida and Moriwaki (1979) undertook radiocarbon dating of the raw flesh and shell of living marine benthic organisms (*Neoliuccinum eatoni, Ophionotus victoriae, Sterechinus neumayeri, Trematomus berunacchii*, and *Zoarcidae* sp.), yielding a mean value of 1120 yr BP; this value is employed as a correction factor in the present study. Before calibrating to calendar ages, we subtracted 1100 years from radiocarbon dates obtained below 180 cm depth in Sk5S and 90 cm depth in Ok5S as a DIC (dissolved inorganic carbon) reservoir correction (Yoshida and Moriwaki, 1979; Hayashi and Yoshida, 1994; Ingolfsson et al., 1998). We did not perform reservoir corrections for radiocarbon dates obtained for sediments from the lacustrine stage, as the carbon residence time is considered to have been negligible for the sediments dated to yield marine DIC reservoir ages. Indeed, the radiocarbon ages of freshwater lacustrine lake sediments in East Antarctica including those at Langhovde, Skarvsnes, and West Ongul Island over the past 2300 years show a linear trend (Matsumoto et al., 2006).

Under these protocols, we obtained ages for the marine-lacustrine transition of 2940±100 cal yr BP for L. Skallen and 1060±90 cal yr BP for L. Oyako, thereby providing emergence ages for these two areas (Fig. 4). Relative sea-level change is recorded in the analyzed lake sediments as a marine-lacustrine transition arising from sea-level change and crustal uplift of the basin sills (Fig. 8). We also estimated the age of the first sediments deposited at the two sites following deglaciation (Figs. 4 and 8). Based on ages obtained for the lowermost sediments in each core, initial sedimentation process started by at least 5293–5559 cal yr BP (2 σ) at L. Skallen and by 1383–1610 cal yr BP (2 σ) at L. Oyako.

3.4 Biological facies of fossil diatoms and the marine-lacustrine transition

The transition from marine to freshwater conditions is clearly documented by sedimentary diatom assemblages in the core from L. Skallen (Fig. 6c), consistent with the geochemical data. Below 200 cm depth in the core, over 70% of the diatoms and other siliceous microfossils are typical of coastal marine taxa, including various *Thalassiosira* species, *Fragilariopsis curta* (Van Heurck) Hustedt, *Amphiprora* sp., numerous *Chaetoceros* spores, and the silicoflaggelate *Distephanus speculum* (Ehrenberg) Haeckel. The freshwater-tolerant taxa within these sediments include *Achnanthidium brevipes* (C. Agardh) Cleve, *Navicula directa* (W. Smith) Ralfs, *Cocconeis imperatrix* M. Peragallo, *Pinnularia quadraterea var. bicuneata* Heiden and Kolbe, and *Amphora* *ovalis* Kützing. Such taxa are typically brackish (Fukushima, 1962), suggesting the influence of coastal/estuarine conditions at some stage during the depositional period.

The relative abundance of estuarine taxa increases at depths of less than 200 cm in the core, coinciding with a decrease in the abundance of marine phytoplankton. Marine taxa are scarce above 175 cm depth, replaced by a predominantly freshwater flora of low diversity. Diversity is lowest in the uppermost sediments (between 15 and 150 cm depth), where diatom assemblages are dominated by *Amphora oligotrophenta* Howarth, *Navicula arcuata* Heiden in Drygalski, and *Navicula molesta* Krasske in Hustedt, with lesser concentrations of *Stauroneis anceps* Ehrenberg, *Diploneis subcincta* (A. Schmidt) Cleve, *Navicula gregaria* Donk in Cleve-Euler, *Achnanthes hankiana* Grunow, and *Amphora ovalis* Kützing. All of these taxa can be found in contemporary lake environments in the Skarvsnes area (Hirano, 1983) and in freshwater creeks in the McMurdo Dry Valleys region of Antarctica (Spaulding et al., 2008).

The transition from marine to freshwater conditions is clearly documented by sedimentary diatom assemblages in the core from L. Skallen (Fig. 6c), consistent with the geochemical data. Below 200 cm depth in the core, over 70% of the diatoms and other siliceous microfossils are typical of coastal marine taxa, including various *Thalassiosira* species, *Fragilariopsis curta* (Van Heurck) Hustedt, *Amphiprora* sp., numerous *Chaetoceros* spores, and the silicoflaggelate *Distephanus speculum* (Ehrenberg) Haeckel. The freshwater-tolerant taxa within these sediments include *Achnanthidium brevipes* (C. Agardh) Cleve, *Navicula directa* (W. Smith) Ralfs, *Cocconeis imperatrix* M. Peragallo, *Pinnularia quadraterea var. bicuneata* Heiden and Kolbe, and *Amphora ovalis* Kützing. Such taxa are typically brackish (Fukushima, 1962), suggesting the influence of coastal/estuarine conditions at some stage during the depositional period.

N. arcuata has been reported from freshwater ponds at Skarvsness (Hirano, 1983) and Akebono Rock (Fukushima et al., 1989), and *N*. *molesta* has been collected from freshwater habitats around the Syowa base of the Ongul Islands (Ko-Bayashi, 1965). However, the dominance of *A. oligotrophenta* in particular might indicate a continuation of brackish conditions through to the present day. *A. oligotrophenta* is considered

BGD

7, 4341–4384, 2010

Crustal uplifting rate associated with late-Holocene glacial-isostatic

Y. Takano et al.

Title Page
Abstract | Introduction
Conclusions | References
Tables | Figures
◀| |▶
◀ ▶
Back | Close
Full Screen / Esc
Printer-friendly Version
Interactive Discussion

a mesohaline diatom, and is cosmopolitan across saline lakes within the European Diatom Database (http://craticula.ncl.ac.uk/Eddi/jsp/index.jsp); however, its abundance appears to be optimal in less-saline waters with a low conductivity (<3 µS/cm). A similar development of *A. oligotrophenta* (described as *A. veneta* and *A. veneta var. capitata*) was observed in the sediments of the coastal brackish Pup Lagoon at Larsemann Hills and interpreted as indicating saline lacustrine conditions following isolation (Gillieson, 1991; Verleyen et al., 2004). The upper sediments of Pup Lagoon is characterized by a ubiquitous cyanobacterial mat that is also evident throughout recent non-marine sediments of L. Skallen. Therefore, it is also possible that the low-diversity flora within the upper sediments of L. Skallen reflect a symbiotic, periphytic relationship between the dominant taxa (*A. oligotrophenta* and *N. arcuata*) and the cyanobacterial mat.

3.5 Phototrophs determined 16S rRNA and the marine-lacustrine transition

The PCR-DGGE analysis was performed to derive independent evidence for changes in the biota of L. Skallen through time based on DGGE band preserved within the sediment profile (Fig. 7). In the region shallower than 190 cm, DGGE band patterns varied according to depth although several bands were detected throughout a broad range of sediment depths. In contrast, sediment samples deeper than 190 cm exhibited almost identical band patterns, characterized by two predominant bands (skA and skB). These two bands had identical nucleotide sequences, which were very closely related to that from the chloroplast of the marine diatom, *Chaetoceros socialis* (identity = 526/528 BP). It is very likely that this sequence originated from marine diatoms buried within the sediment. Marine diatom related bands were not detected in the shallower layers, suggesting a change in the biota of L. Skallen Oike through time. Band skC was detected in the depth range of 160 to 200 cm, and closely related to cyanobacteria of the genus *Synechococcus*. It is likely that the organism corresponding to this band existed within the water column or surface sediments during the depositional age corresponding to these layers. However, the other sequenced DGGE bands (labeled in Fig. 7) were closely related to heterotrophic bacteria or only distantly related to cultured bacterial strains. As to these bands, it is impossible to judge whether they had been preserved in the sediment since their deposition, or were actively growing within the sediment.

4 Discussion

4.1 Holocene crustal uplift rate around Lützow-Holm Bay

Model predictions of crustal motions and gravity changes driven by glacial isostatic adjustment (GIA) in West Antarctica indicate present-day peak GIA-related uplift rates of 14–18 mm yr^{-1} (e.g. Ellsworth Mountains region), with lower rates in the East Antarctic coastal region (Ivins and James, 2005). However, few studies have documented the emergence age of marine-lacustrine transitions in Antarctica. In the Lambert Glacier region, the relative uplifting rate and emergence age of Heart Lake and Pup Lagoon (in the Larsemann Hills) have been estimated to be 1.8–1.9 mm yr^{-1} based on a linear extrapolation of dated marine-lacustrine transitions over the past 2800 cal yr BP (Verleyen et al., 2005). This figure is comparable to rates reported for the Vestfold Hills (Zwartz et al., 1998).

Based on comprehensive descriptions for the altitudes of present-day lakes, age determinations of the marine-lacustrine transitions at Lakes Skallen and Oyako (Fig. 9a), and possible off-set model from ecology in *L. elliptica* (Fig. 10), we estimate the mean crustal uplifting rates during the late Holocene in the Lützow-Holm Bay area. Here we consider a scheme for calculating the crustal uplifting rate, where t is defined as time in chronological order. The time t_0 represents the initial marine stage, and t_1 and t_2 represent the emergence age (i.e., the transition from marine to freshwater; $\text{a.m.s.l.}_{t=1}$) and the present day ($\text{a.m.s.l.}_{t=2}$), respectively (Fig. 8). Therefore, the crustal uplifting rate k is defined as

$$k = (\text{a.m.s.l.}_{t=2} - \text{a.m.s.l.}_{t=1})/(t_2 - t_1)$$

where a.m.s.l.$_{t=1}$ is equal to 0 m, representing the emergence event (marine-lacustrine transition) in time units of cal yr BP. Given that the present sill heights for L. Skallen and L. Oyako are 10 and 5 m a.m.s.l., respectively, the mean crustal uplifting rate $k_{\mathrm{Sk,Ok}}$ (accuracy <0.5 m; see Aoki et al., 2000) is calculated to be 3.6 mm yr^{-1} (r^2=0.97) for the period since the marine-lacustrine transition; i.e., over the past 2940 years at Skallen and past 1060 years at Skarvsnes (Eq. 3 in Fig. 9a).

The relative sea-level curve of the Vestfold Hills was estimated from marine-lacustrine transition by Ace Lake, Anderson Lake, Highway Lake, Watts Lake, and Organic Lake (Roberts and McMinn, 1999; Zwartz et al., 1998). Subsequently, the relative sea-level curve of the Larsemann Hills was also estimated using data from Kirisjes Pond, Heart Lake, and Pup Lagoon (Verleyen et al., 2005). Hence, comparison of relative sea-level changes with other ice-free areas along the EAIS suggests that the present uplifting rate along the Soya Coast is greater than that in the Larsemann Hills and Vestfold Hills (Fig. 11).

4.2 Ecology of the suspension feeder bivalve, *L. elliptica*: an insight into habitat depth

In order to validate the first-order model of glacial-isostatic uplift rate derived from L. Skallen and L. Oyako ($k_{\mathrm{Sk,Ok}}$), we compared these estimates with uplift rates based on radiocarbon dating of in situ marine mollusk fossils (*L. elliptica*) from raised beach deposits, described previously (Miura et al., 1998c) (Figs. 9 and 10). Radiocarbon dating of marine fossils around Antarctica is problematic because of the reservoir effect associated with melt water from the ice sheet and upwelling of Antarctic deep water. Furthermore, we cannot confirm the water depth of the habitat of marine fossils that lived below the paleo-sea level at which carbon fixation within indigenous shells occurred. Therefore, it is useful to consider the ecology and habitat preferences of *L. elliptica* prior to interpreting the radiocarbon composition of fossil remains. The estimated glacial-isostatic uplift rate presented above can be complemented by a re-assessment of radiocarbon dates obtained previously for the marine mollusk *L. elliptica* fossils (Miura et al., 1998c).

L. elliptica is an endemic suspension feeder that is probably most common in water depths shallower than 20 m (Dell, 1990). It is widely distributed around Antarctica, occurring as dense patches in subtidal (sub-littoral zone) soft-sediment areas, and is one of the most conspicuous members of infaunal assemblages (e.g. Ahn, 1993; Urban and Mercuri, 1998; Jonkers, 1999; Cattaneo-Vietti et al., 2000; Ahn, 2001; Ahn et al., 2004; Norkko et al., 2004; Sato-Okoshi and Okoshi, 2008; Tatian et al., 2008). The vertical and spatial distribution of *L. elliptica* is mainly controlled by habitat stability and food availability in benthic environments (Ahn et al., 2003). In a study conducted at King George Island, Ahn (1994) reported that *L. elliptica* began to appear in the subtidal zone (depth >6–7 m) on the gentle slope. Ahn and co-workers estimated *L. elliptica* biomass at different water depths at several shore localities in Antarctica.

Ice impact in areas near intertidal (littoral) zones is a prevailing physical factor that affects the vertical distribution of *L. elliptica*. Below the ice-impact zone, optimum biological interactions (including the light regime and primary production) act as the main structuring force on the benthic community (Ahn, 1994; Ahn and Shim, 1998; Sahade et al., 1998). *L. elliptica* lives buried in the sediment (burrowing depth >50 cm) with the aid of large siphons, and reaches a length of approximately 100 mm over 12–13 years (Ralph and Maxwell, 1977; Zamorano et al., 1986). Since species-specific and region-specific corrections have not yet been developed, we applied the general pre-bomb marine reservoir correction of 1300 years to the radiocarbon ages, following previous studies using emerged Antarctic marine fossils (Berkman et al., 1998). Considering this ecological context, we propose that the habitat depth of *L. elliptica* (below sea-level: meter, corresponding to life position within the subtidal water column), in combination with its burrowing depth (below the sea floor: meter, corresponding to siphon length > ca. 0.5 m) yields a depth offset showing ΔH (Fig. 10), which in turn yields (ΔT) an age offset with regard to the calendar age model (Fig. 9b).

4.3 Validity of linear approximation model of marine-lacustrine emergence age

Miura et al. (1998c) compiled the ages of emerged beaches based on radiocarbon dating of *L. elliptica* fossils from along the Soya Coast, and reported two clusters of ages: a younger mid-Holocene group (3000–8000 yr BP, uncorrected for reservoir effects) and an older late-Pleistocene group (Fig. 9b). Nakada et al. (2000) examined sea-level variations at eight sites along the coast of Antarctica with the aim of reconstructing the melting history of the Antarctic ice sheet. These earlier studies were limited by uncertainty regarding the magnitude of Antarctic reservoir effects, especially for the late Holocene before ca. 3000 yr BP.

To estimate relative sea-level change for a previously neglected period during the past 3000 yr BP, we fitted a linear approximation model (Fig. 9a) with an emergence age based on the ages obtained for the marine-lacustrine transitions and the ages of in situ *L. elliptica* collected from Skarvsnes and Langhovde (Maemoku et al., 1997; Miura et al., 1998a, b, c), calibrated using a calcareous marine reservoir correction (Berkman et al., 1998). Bearing in mind the above ecological description of the living environment of *L. elliptica*, we interpreted the offset of chronological time and sea-level record of *L. elliptica* using Eqs. (2) and (3) (Fig. 9). The maximum possible water depth of the subtidal environment is represented as the difference between the value of a.m.s.l. on Eqs. (2) and (3) in the a.m.s.l. (m) axis (ΔH: habitat depth below sea-level and below the sea floor during the lifecycle of *L. elliptica* with thickness of re-deposition sediment). The resulting emergence age (cal yr BP) gives a crustal uplifting rate $k_{\mathrm{Sk,Ok}}$ of 3.6 mm yr^{-1} (r^2=0.97, this study). Based on a linear approximation model (Fig. 9b), we propose $k_{L.\ elliptica\ (1)}$ and $k_{L.\ elliptica\ (2)}$ (rate constant k of Eqs. 1 and 2, respectively) to be 3.9 mm yr^{-1} (r^2=0.68) and 3.2 mm yr^{-1}(r^2=0.68), respectively. Hence, the burial age (ΔT) of fossilized *L. elliptica* would correspond to the difference between Eqs. (2) and (3) along the time (cal yr BP) axis (see Fig. 10). Although we cannot confirm the precise paleo-sealevel values associated with *L. elliptica* and its exact marine reservoir effect (e.g. Hayashi and Yoshida, 1994; Berkman et al., 1998; Ingolfsson et al., 1998), we presume that the linear approximation obtained between emergence age (Fig. 9a) and *L. elliptica* age (Fig. 8b; Miura et al., 1998c) represents the mean uplifting rate associated with regional isostatic rebound during the late Holocene.

5 Conclusions

In a study of the Soya Coast, Lützow-Holm Bay, East Antarctica, we investigated the sedimentary facies, biological facies, and crustal uplift rates based on the timing of marine-lacustrine transitions associated with regional glacio-isostatic rebound during Holocene deglaciation in EAIS. A combination of inorganic geochemistry and nitrogen isotope analysis of organic matter, supplemented by diatom species assemblages and fossil DNA and 16S rRNA for Lake Skallen, clearly document a transition from a marine to freshwater aquatic environment in both lakes, with the transition occurring in 2940±100 cal yr BP at L. Skallen and 1060±90 cal yr BP at L. Oyako. Based on these estimates, the crustal uplift rate of the Soya Coast was faster than other ice-free areas such as Lambert glacier region and Vestfold Hills. These differences are probably due to differing geological settings: the late Holocene deglaciation was the primary factor in controlling the emergence of Lützow-Holm Bay region and also in generating simultaneous changes in sedimentary and biological facies. Our estimate of the crustal uplift rate is supported by a regional survey of radiocarbon dates of fossils of the endemic suspension feeder *L. elliptica*. An improved understanding of the ecology of these organisms would represent a key advance in integrating geological and geochemical age models for the precise determination of the rate and extent of crustal uplift during the late Holocene.

Acknowledgements. We thank S. Okamura (Geograph. Surv. Institute), S. Sakanaka (Akita University), T. Irino (Hokkaido University) for discussion, S. Imura (Natl. Inst. Polar Res., NIPR) and K. Seto (Shimane University) for logistical support, H. Miura (NIPR) and G. Matsumoto-Inoue (Otsuma Women Univ.) for reviewing the manuscript, and the members of the summer party of the 47th Japan Antarctica Research Expedition (K. Shiraishi) for their assistance. AMS experiments were partly supported by H. Matsuzaki (University Tokyo). The assistance of E. Takeda (Hokkaido University) with microbial community analysis, M. Saito-Kato (Natl. Museum, Japan) and R. Jordan (Yamagata University) with diatom taxonomy and the provision of reference materials is greatly appreciated, as is the contribution of S. Darroch (Tokyo University) for assistance in the preparation of diatom slides. This research was supported in part by the Japan Society for the Promotion of Science (Y.T, N.O, and J.J.T), the Global Environment Research Fund (Y.Y) and REGAL project of NIPR (S. Imura and H. Kanda). The present research activities were also collaborative work during International Polar Year (IPY 2007–2008).

References

Ahn, I. Y.: Enhanced particle flux through the biodeposition by the Antarctic suspension-feeding bivalve *Laternula elliptica* in Marian Cove, King George Island, J. Exp. Mar. Biol. Ecol., 171, 75–90, 1993.

Ahn, I. Y.: Ecology of the Antarctic bivalve *Laternula elliptica* (King and Broderip) in Collins Harbor, King George Island: benthic environment and an adaptive strategy, Memoir Natl. Inst. Polar Res., 50, 1–10, 1994.

Ahn, I. Y. and Shim, J. H.: Summer metabolism of the Antarctic clam, *Laternula elliptica* (King and Broderip) in Maxwell Bay, King George Island and its implications, J. Exp. Mar. Biol. Ecol., 224, 253–264, 1998.

Ahn, I. Y., Chung, H., and Choi, K. S.: Some ecological and physiological features of the Antarctic clam, *Laternula elliptica* (King and Broderip) in a nearshore habitat on King George Island, Ocean Polar Res., 23, 419–424, 2001.

Ahn, I. Y., Kang, J., and Kim, K.-W.: The effect of body size on metal accumulations in the bivalve *Laternula elliptica*, Antarct. Sci., 13, 355–362, 2004.

Ahn, I. Y., Surh, J., Park, Y. G., Kwon, H., Choi, K. S., Kang, S. H., Choi, H. J., Kim, K. W., and Chung, H.: Growth and seasonal energetics of the Antarctic bivalve *Laternula elliptica* from King George Island, Antarctica, Mar. Ecol. Prog.-Ser., 257, 99–110, 2003.

Anderson, J. B., Shipp, S. S., Lowe, A. L., Wellner, J. S., and Mosola, A. B.: The Antarctic ice sheet during the Last Glacial Maximum and its subsequent retreat history: a review, Quaternary Sci. Rev., 21, 49–70, 2002.

Aoki, S., Ozawa, T., Doi, K., and Shibuya, K.: GPS observation of the sea level variation in Lützow-Holm Bay, Antarctica, Geophys. Res. Lett., 27, 2285–2288, 2000.

Battarbee, R. W., Jones, V. J., Flower, R. J., Cameron, N. G., Bennion, H., Carvalho, L., and Juggins, S.: Diatoms, in: Tracking environmental change using lake sediments volume 3: terrestrial, algal and siliceous indicators, edited by: Smol, J. P., Birks, H. J. B., and Last, W. M., Kluwer, Dordrecht, 2001.

Bentley, M. J.: Volume of Antarctic Ice at the Last Glacial Maximum, and its impact on global sea level change, Quaternary Sci. Rev., 18, 1569–1595, 1999.

Berkman, P. A. and Forman, S. L.: Pre-bomb radiocarbon and the reservoir correction for calcareous marine species in the Southern Ocean, Geophys. Res. Lett., 23, 363–366, 1996.

Berkman, P. A., Andrews, J. T., Bjorck, S., Colhoun, E. A., Emslie, S. D., Goodwin, I. D., Hall, B. L., Hart, C. P., Hirakawa, K., Igarashi, A., Ingolfsson, O., Lopez-Martinez, J., Lyons, W. B., Mabin, M. C. G., Quilty, P. G., Taviani, M., and Yoshida, Y.: Circum-Antarctic coastal environmental shifts during the Late Quaternary reflected by emerged marine deposits, Antarct. Sci., 10, 345–362, 1998.

Cattaneo-Vietti, R., Chiantore, M., Schiaparelli, S., and Albertelli, G.: Shallow- and deep-water mollusc distribution at Terra Nova Bay (Ross Sea, Antarctica), Polar Biol., 23, 173–182, 2000.

Cortese, G., Gersonde, R., Hillenbrand, C. D., and Kuhn, G.: Opal sedimentation shifts in the World Ocean over the last 15 M yr, Earth Planet. Sc. Lett., 224, 509–527, 2004.

Dell, R. K.: Antarctic mollusca: with special reference to the fauna of Ross Sea, B. Roy. S. NZ., 27, 1–311, 1990.

Fukushima, H., Ko-Bayashi, T., and Ishida, H.: Diatoms from Akebono Rock in Antarctica. Abstract, Twelfth Symposium on Polar Biology, National Institute of Polar Research, Tokyo, Japan, 1989.

Fukushima, H.: Notes on diatom vegetation of the Kasumi Rock ice free area, Prince Olav Coast, Antarctica, Antarct. Rec., 15, 1267–1280, 1962.

Fukuzaki, Y., Shibuya, K., Doi, K., Ozawa, T., Nothnagel, A., Jike, T., Iwano, S., Jauncey, D. L., Nicolson, G. D., and McCulloch, P. M.: Results of the VLBI experiments conducted with Syowa Station, Antarctica, J. Geodesy, 79, 379–388, 2005.

Geographical Survey Institute: Skallen, Map compilation from air photography of 21 Jan 1969, controlled by triangulation points established by JARE, 1969, 1973.

Geographical Survey Institute: Skarvsnes: the principan part, Map compilation from air photographs of 1962, 1969 and 1971, controlled by triangulation points established by JARE, 1969, 1970 and 1973, 1987.

Gillieson, D. S.: An environmental history of two freshwater lakes in the Larsemann Hills, Antarctica, Hyrobiologia, 214, 327–331, 1991.

Hayashi, M. and Yoshida, Y.: Holocene raised beaches in the Lützow-Holm Bay region, East Antarctica, Memoir Natl. Inst. Polar Res., 50, 49–84, 1994.

Hirano, M.: Freshwater algae from Skarvsness, near Syowa station, Antarctica, Memoir Natl. Inst. Polar Res. Ser. E, 35, 1–29, 1983.

Hughen, K. A., Baillie, M. G. L., Bard, E., Beck, J. W., Bertrand, C. J. H., Blackwell, P. G., Buck, C. E., Burr, G. S., Cutler, K. B., Damon, P. E., Edwards, R. L., Fairbanks, R. G., Friedrich, M., Guilderson, T. P., Kromer, B., McCormac, G., Manning, S., Ramsey, C. B., Reimer, P. J., Reimer, R. W., Remmele, S., Southon, J. R., Stuiver, M., Talamo, S., Taylor, F. W., der Plicht, J., and Weyhenmeyer, C. E.: Marine04 marine radiocarbon age calibration, 0–26 cal kyr BP, Radiocarbon, 46, 1059–1086, 2004.

Huybrechts, P.: Sea-level changes at the LGM from ice-dynamic reconstructions of the Greenland and Antarctic ice sheets during the glacial cycles, Quaternary Sci. Rev., 21, 203–231, 2002.

Igarashi, A., Numanami, H., Tsuchiya, Y., Harada, N., Fukuchi, M., and Saito, T.: Radiocarbon ages of Molluscan shell fossils in raised beach deposits along the east coast of Lützow-Holm Bay, Antarctica, determined by Accelerator mass-spectrometry: Proc. NIPR Symp. Polar Biol., 8, 154–162, 1995.

Imai, N., Terashima, S., Itoh, S., and Ando, A.: 1998 compilation of analytical data for five GSJ geochemical reference samples, Geostandard. Newslett., 23, 223–250, 1999.

Imai, N., Terashima, S., Itoh, S., and Ando, A.: 1996 compilation of analytical data on nine GSJ geochemical reference samples, ”Sedimentary rock series”, Geostandard. Newslett., 20, 165–216, 1996.

Imai, N., Terashima, S., Itoh, S., and Ando, A.: 1994 Compilation Values for Gsj Reference Samples, Igneous Rock Series, Geochem. J., 29, 91–95, 1995.

Imura, S., Bando, T., Seto, K., Ohtani, S., Kudoh, S., and Kanda, H.: Distribution of aquatic mosses in the Soya Coast region, East Antarctica, Polar Biosci., 16, 1–10, 2003.

Ingolfsson, O., Hjort, C., Berkman, P. A., Bjorck, S., Colhoun, E., Goodwin, I. D., Hall, B., Hirakawa, K., Melles, M., Moller, P., and Prentice, M. L.: Antarctic glacial history since the Last Glacial Maximum: an overview of the record on land, Antarct. Sci., 10, 326–344, 1998.

Ivins, E. R. and James, T. S.: Antarctic glacial isostatic adjustment: a new assessment, Antarct. Sci., 17, 541–553, 2005.

James, T. S. and Ivins, E. R.: Predictions of Antarctic crustal motions driven by present-day ice sheet evolution and by isostatic memory of the Last Glacial Maximum, J. Geophys. Res., 103, 4993–5017, 1998.

Jonkers, H.A.: Aligned growth positions in Pliocene *Laternula elliptica* (King Camp; Broderip) (Bivalvia: Anomalodesmata: Laternulidae), Antarct. Sci., 11, 463–464, 2004.

Kaminuma, K.: On the possibility of detecting absolute crustal uplift at Syowa station, Antarctica, Proc. NIPR Symp. Antarct. Geosci., 9, 16–23, 1996.

Kawakami, T. and Motoyoshi, Y.: Timing of attainment of the spinel + quartz coexistence in garnet-sillimanite leucogneiss from Skallevikshalsen, Lützow-Holm complex, East Antarctica, J. Miner. Petrol. Sci., 99, 311–319, 2004.

Ko-Bayashi, T.: Variations on some pinnate diatoms from Antarctica, Japanese Antarctic Research Expedition Scientific Reports, Series E, No. 24, 1965.

Krammer, K. and Lange-Bertalot, H.: *Bacillariophyceae*, 1. Teil: *Naviculaceae*, Gustav Fischer Verlag, Stuttgart, New York, 1986.

Krammer, K. and Lange-Bertalot, H.: *Bacillariophyceae*, 2. Teil: *Bacillariaceae, Epithemiaceae, Surriellaceae*, Gustav Fischer Verlag, Jena, 1988.

Krammer, K. and Lange-Bertalot, H.: *Bacillariophyceae*, 3. Teil: *Centrales, Fragilariaceae, Eunotiaceae*, Gustav Fischer Verlag, Stuttgart, Jena, 1991a.

Krammer, K. and Lange-Bertalot, H.: *Bacillariophyceae*, 4. Teil: *Achnanthaceae*, Kritische Ergänzungen zu *Navicula (Lineolatae)* und *Gomphonema*, Gesamtliteraturverzeichnis Teil 1–4, Gustav Fischer Verlag, Stuttgart, Jena. , 1991b.

Lambeck, K.: Glacial rebound and sea-level change – an example of a relationship between mantle and surface processes, Tectonophy, 223, 15–37, 1993.

Maemoku, H., Miura, H., Saigusa, S., and Moriwaki, K.: Stratigraphy of the late Quaternary raised beach deposits in the northern part of Langhovde, Lützow-Holm bay, East Antarctica, Proc. NIPR Symp. Antarct. Geosci., 10, 178–186, 1997.

Matsumoto, G. I., Komori, K., Enomoto, A., Imura, S., Takemura, T., Ohyama, Y., and Kanda, H.: Environmental change in Syowa station area of Antarctica during the last 2300 years inferred from organic components in lake sediment cores, Polar Biosci., 19, 51–62, 2006.

Medlin, L. K. and Priddle, J.: Polar marine diatoms, British Antarctic Survey, Natural Environmental Council, Cambridge, 1990.

Miura, H., Moriwaki, K., Maemoku, H., and Hirakawa, K.: Fluctuations of the East Antarctic ice-sheet margin since the last glaciation from stratigraphy of raised beach deposits along the Soya coast, Ann. Glaciol., 27, 297–301, 1998a.

Miura, H., Maemoku, H., Seto, K., and Moriwaki, K.: Late Quaternary East Antarctic melting event in the Soya Coast region based on stratigraphy and oxygen isotopic ratio of fossil mollusks, Polar Geosci., 11, 260–274, 1998b.

Miura, H., Maemoku, H., Igarashi, A., and Moriwaki, K.: Late Quaternary raised beach deposits and radiocarbon dates of marine fossils around Lützow-Holm Bay, Special Map Ser. Natl. Inst. Polar Res., 6, 1–46, 1998c.

Muyzer, G., Brinkhoff, T., Nübel, U., Santegoeds, C., Schafer, H., and Wawer, C.: Denaturing gradient gel electrophoresis (DGGE) in microbial ecology, in: Molecular Microbial Ecology Manual, 3rd ed.ition, editdt by: Akkermans, A. D. L., van Elsas, J. D., and de Bruijn, F. J., Kluwer Academic Publishers, Dordrecht, The Netherlands, 3.4.4, 1–27, 1996.

Nakada, M. and Lambeck, K.: Late Pleistocene and Holocene sea-level change in the Australian region and mantle rheology, Geophys. J. Oxford, 96, 497–517, 1989.

Nakada, M., Kimura, R., Okuno, J., Moriwaki, K., Miura, H., and Maemoku, H.: Late Pleistocene and Holocene melting history of the Antarctic ice sheet derived from sea-level variations, Mar. Geol., 167, 85–103, 2000.

Norkko, J., Norkko, A., Thrush, S. F., and Cummings, V. J.: Detecting growth under environmental extremes: spatial and temporal patterns in nucleic acid ratios in two Antarctic bivalves, J. Exp. Mar. Biol. Ecol., 326, 144–156, 2005.

Ohkouchi, N., Nakajima, Y., Okada, H., Ogawa, N. O., Suga, H., Oguri, K., and Kitazato, H.: Biogeochemical processes in the saline meromictic Lake Kaiike, Japan: implications from molecular isotopic evidences of photosynthetic pigments, Environ. Microbiol., 7, 1009–1016, 2005.

Ohzono, M., Tabei, T., Doi, K., Shibuya, K., and Sagiya, T.: Crustal movement of antarctica and syowa station based on GPS measurements, Earth Planets Space, 58, 795–804, 2006.

Oyama, M. and Takehara, H.: Revised Standard Soil Color Charts, 27th edition edited by: The Ministry of Agriculture, Forestry and Fisheries of Japan, 2005.

Ralph, R. and Maxwell, J. G. H.: Growth of two Antarctic lamellibranchs: Adamussium colbecki and *Laternula elliptica*, Mar. Biol., 42, 171–175, 1977.

Reimer, P. J., Baillie, M. G. L., Bard, E., Bayliss, A., Beck, J. W., Bertrand, C. J. H., Blackwell, P. G., Buck, C. E., Burr, G. S., Cutler, K. B., Damon, P. E., Edwards, R. L., Fairbanks, R. G., Friedrich, M., Guilderson, T. P., Hogg, A. G., Hughen, K. A., Kromer, B., McCormac, G., Manning, S., Ramsey, C. B., Reimer, R. W., Remmele, S., Southon, J. R., Stuiver, M., Talamo, S., Taylor, F. W., van der Plicht, J., and Weyhenmeyer, C. E.: IntCal04 terrestrial radiocarbon age calibration, 0–26 cal kyr BP, Radiocarbon, 46, 1029–1058, 2004.

Roberts, D. and McMinn, A.: A weighted-averaging regression and calibration model for inferring lakewater salinity from fossil diatom assemblages in saline lakes of the Vestfold Hills: a new tool for interpreting Holocene lake histories in Antarctica, J. Paleolimnol., 19, 99–113, 1998.

Sahade, R., Tatian, M., Kowalke, J., Kuhne, S., and Esnal, G. B.: Benthic faunal associations on soft substrates at Potter Cove, King George Island, Antarctica, Polar Biol., 19, 85–91, 1998.

Sato-Okoshi, W. and Okoshi, K.: Characteristics of shell microstructure and growth analysis of the Antarctic bivalve *Laternula elliptica* from Lützow-Holm Bay, Antarctica, Polar Biol., 31, 131–138, 2008.

Sawagaki, T. and Hirakawa, K.: Erosion of bedrock by subglacial meltwater, Soya Coast, East Antarctica, Geogr. Ann. A, 79A, 223–238, 1997.

Shibuya, K., Doi, K., and Aoki, S.: Ten years' progress of Syowa Station, Antarctica, as a global geodesy network site, Polar Geosci., 16, 29–52, 2003.

Soudarin, L., Cretaux, J. F., and Cazenave, A.: Vertical crustal motions from the DORIS space-geodesy system, Geophys. Res. Lett., 26, 1207–1210, 1999.

Spaulding, S., Esposito, R., Lubinski, D., Horn, S., Cox, M., McKnight, D., Alger, D., Hall, B., Mayernick, M., Whittaker, T., and Yang, C.: Antarctic freshwater diatoms web site, McMurdo Dry Valleys LTER, http:/huey.colorado.edu/diatoms, last access: 1 June 2010, 2008.

Stuiver, M. and Reimer, P. J.: Extended C-14 Data-Base and Revised Calib 3.0 C-14 Age Calibration Program, Radiocarbon, 35, 215–230, 1993.

Stuiver, M., Reimer, P. J., and Braziunas, T. F.: High-precision radiocarbon age calibration for terrestrial and marine samples, Radiocarbon, 40, 1127–1151, 1998.

Tanabe, Y., Kudoh, S., Imura, S., and Fukuchi, M.: Phytoplankton blooms under dim and cold conditions in freshwater lakes of East Antarctica, Polar Biol., 31, 199–208, 2008.

Tatian, M., Sahade, R., Mercuri, G., Fuentes, V., Antacli, J., Stellfeldt, A., and Esnal, G.: Feeding ecology of benthic filter-feeders at Potter Cove, an Antarctic coastal ecosystem, Polar Biol., 31, 509–517, 2008.

Urban, H.-J. O. R. and Mercuri, G.: Population dynamics of the bivalve *Laternula elliptica* from Potter Cove, King George Island, South Shetland Islands, Antarct. Sci., 10, 153–160, 1998.

Verleyen, E., Hodgson, D. A., Milne, G. A., Sabbe, K., and Vyverman, W.: Relative sea-level history from the Lambert Glacier region, East Antarctica, and its relation to deglaciation and Holocene glacier readvance, Quarternary Res., 63, 45–52, 2005.

Verleyen, E., Hodgson, D. A., Sabbe, K., Vanhoutte, K., and Vyverman, W.: Coastal oceanographic conditions in the Prydz Bay region (East Antarctica) during the Holocene recorded in an isolation basin, The Holocene, 14, 246–257, 2004.

Yokoyama, Y., Lambeck, K., De Deckker, P., Johnston, P., and Fifield, L. K.: Timing of the Last Glacial Maximum from observed sea-level minima, Nature, 406, 713–716, 2000.

Yokoyama, Y., Purcell, A., Marshall, J., and Lambeck, K.: Sea-level during the early deglaciation period in the Great Barrier Reef, Australia, Global Planet. Change, 53, 147–153, 2006.

Yokoyama, Y., Miyairi, Y., Matsuzaki, H., and Tsunomori, F.: Relation between acid dissolution time in the vacuum test tube and time required for graphitization for AMS target preparation, Nucl. Instrum. Meth. B, 259, 330–334, 2007.

Yoshikawa, T. and Toya, H.: Report on Geomorphological results of the Japanese Antarctic Research Expedition, 1956–1957, Antarct, Record (Nankyoku Siryo), 1, 1–13, 1957.

Yoshida, Y. and Moriwaki, K.: Some Consideration on Elevated Coastal Features and Their Dates around Syowa Station, Antarctica, Memoirs Natl. Inst. Polar Res., 13, 220–226, 1979.

Zamrano, J., Duarte, E. W., and Moreno, A. C.: Predation upon *Laternula elliptica* (Bivalvia, Anatinidae): A field manipulation in South Bay, Antarctica, Polar Biol., 6, 139–143, 1986.

Zwartz, D., Bird, M., Stone, J., and Lambeck, K.: Holocene sea-level change and ice-sheet history in the Vestfold Hills, East Antarctica, Earth Planet. Sc. Lett., 155, 131–145, 1998.

Table 1. Details of sampling locations, lake characteristics, and coring sites. The primary information of a.m.s.l. (m) of two lakes was documented by Imura et al. (2003), Geographical Survey Institute (1973) and Geographical Survey Institute (1987).

Sampling location and lake profile				Sample profile		Coring point (GPS data)	
Area	Lake Name	Altitude (a.m.s.l.)	Max depth	Sample name	Core length	Latitude (S)	Longitude (E)
Skallen	L. Skallen Ôike	10 m	8.5 m	Sk5S	362 cm	69.40′17.8″	39.24′44.0″
Skarvsnes	L. Oyako	5 m	8.0 m	Ok5S	153 cm	69.28′31.0″	39.36′08.23″

Table 2. Radiocarbon (^{14}C) age data obtained by accelerator mass spectrometry (AMS) for organic carbon fractions from cores Sk5S and Ok5S collected from L. Skallen and L. Oyako, respectively. Conventional radiocarbon dating of organic carbon ($^{14}C_{org}$, yr BP) and correction for the marine reservoir effect (ΔR as 1100 yr for marine stage sequence; 360–362 cm in Sk5S; 150–153 cm in Ok5S) are based on previous studies (Yoshida and Moriwaki, 1979; Hayashi and Yoshida, 1994; Ingolfsson et al., 1998). Calendar age data were calculated using the calibration program Calib Rev 5.0.1 (Stuiver et al., 1993, 1998) for INTCAL and MARINE (Hughen et al., 2004; Reimer et al., 2004). The $^{14}C_{org}$ age of marine-lacustrine transition sequence (180–190 cm in Sk5S; 90–95 cm in Ok5S) were calculated by the linear extrapolation between marine and lacustrine data (Fig. 4). The marine carbon percentages we used at the marine-lacustrine transition sequence (180–190 cm in Sk5S; 90–95 cm in Ok5S) and marine stage sequence (360–362 cm in Sk5S; 150–153 cm in Ok5S) were 50% and 100% in the calibration program, respectively.

L. Skallen	Depth (cm)	Mid-depth	Conventional radiocarbon age (δ^{13}C corrected) (yr BP)	1 σ ±	Calendar age (2 σ range) (cal yr BP)	Relative area under probability function
Sk5S	70–80	75.0	1285	40	1167–1294	0.93
					1132–1162	0.05
					1091–1108	0.02
	150–160	155.0	2580	40	2691–2769	0.67
					2612–2638	0.12
					2498–2596	0.21
	180–190	185.0	4150	40	2843–3042	0.96
					2800–2820	0.02
					3046–3063	0.02
	360–362	361.0	6160	60	5293–5559	1.00
L. Oyako Ok5S	36–39	37.5	435	30	456–532	0.97
					337–348	0.03
	80–85	82.5	965	40	788–939	0.98
					943–955	0.02
	90–95	92.5	2010	40	965–1150	0.95
					1156–1171	0.05
	150–153	151.5	3050	40	1383–1610	1.00

Table 3. Concentrations of major elements (MgO, Al_2O_3, SiO_2, K_2O, CaO, TiO_2, MnO, and Fe_2O_3; average values of duplicate analyses), total carbon (TC), total nitrogen (TN), and total sulfur (TS) in core Sk5S recovered from L. Skallen.

Depth	Mid-depth	MgO	Al_2O_3	SiO_2	K_2O	CaO	TiO_2	MnO	Fe_2O_3	Carbon	Nitrogen	Sulfur	C/N
(cm)						(wt%)					(wt%)		
0–10	5.0	1.23	3.63	33.2	1.49	2.32	0.38	0.10	14.73	17.8	1.5	1.7	11.5
10–20	15.0	1.23	4.00	33.1	1.69	2.32	0.44	0.11	14.75	13.0	1.3		10.4
20–30	25.0	0.86	3.45	29.5	1.74	2.41	0.43	0.10	9.52	16.1	1.6	1.8	10.2
30–40	35.0	1.01	3.45	31.1	1.84	2.48	0.44	0.09	7.67	19.1	1.7		11.4
40–50	45.0	0.82	4.24	30.0	1.94	2.50	0.50	0.10	10.06	19.7	1.8	1.5	11.1
50–60	55.0	1.08	3.72	27.3	1.78	2.41	0.44	0,.1	11.82	17.7	1.6		11.2
60–70	65.0	1.74	4.37	29.7	2.03	2.45	0.52	0.10	9.56	18.4	1.7	1.7	10.6
70–80	75.0	1.55	4.00	32.3	1.96	2.46	0.50	0.09	8.25	17.9	1.6		11.5
80–90	85.0	0.59	3.88	30.8	1.83	2.36	0.45	0.09	7.07	15.2	1.3	1.7	11.4
90–100	95.0	0.77	3.80	32.0	1.91	2.49	0.48	0.09	6.67	15.3	1.4		11.1
100–110	105.0	0.96	4.10	33.0	1.66	2.24	0.41	0.08	9.68	13.0	1.2	9.0	10.8
110–120	115.0	1.44	5.02	36.2	1.86	2.29	0.45	0.08	9.56	14.2	1.3		10.9
120–130	125.0	0.91	4.38	36.4	1.63	2.25	0.39	0.08	8.97	14.2	1.3	7.2	11.1
130–140	135.0	1.27	5.40	43.1	1.90	2.43	0.47	0.08	7.37	11.7	1.1		11.1
140–150	145.0	1.16	4.70	41.1	1.78	2.33	0.43	0.08	6.92	15.0	1.3	7.0	11.6
150–160	155.0	2.39	5.40	45.4	1.98	2.47	0.49	0.08	7.36	11.1	1.0		10.8
160–170	165.0	2.10	6.76	45.9	2.17	2.83	0.54	0.09	6.32	8.6	0.7	3.4	11.8
170–180	175.0	1.35	5.43	52.5	1.87	2.82	0.46	0.09	5.50	7.9	0.6		14.1
180–190	185.0	0.81	6.05	60.5	1.82	2.48	0.46	0.06	4.81	2.9	0.3	2.0	8.8
190–200	195.0	1.36	6.84	58.5	2.03	2.58	0.50	0.07	4.75	2.7	0.3		8.9
200–210	205.0	0.67	5.08	62.5	1.66	2.31	0.42	0.06	4.12	3.0	0.4	1.6	8.5
210–220	215.0	0.88	4.12	62.7	1.56	2.18	0.39	0.05	4.36	3.3	0.4		9.4
220–230	225.0	0.88	5.10	63.6	1.77	2.28	0.45	0.06	4.86	3.4	0.4	2.0	9.3
230–240	235.0	1.20	4.92	64.1	1.66	2.22	0.41	0.06	4.66	3.8	0.4		9.1
240–250	245.0	0.18	3.17	69.7	1.24	2.01	0.27	0.04	3.35	3.2	0.4	1.4	9.1
250–260	255.0	0.55	4.67	68.0	1.46	2.40	0.37	0.05	4.00	2.3	0.3		8.1
260–270	265.0	0.09	3.27	68.3	1.36	2.02	0.32	0.05	3.94	3.1	0.4	1.6	8.1
270–280	275.0	0.99	4.27	66.9	1.52	2.16	0.39	0.33	4.25	2.4	0.3		8.6
280–290	285.0	0.04	1.17	73.4	0.91	1.77	0.20	0.03	2.71	3.3	0.4	1.1	8.8
290–300	295.0	0.00	1.64	73.1	0.98	1.78	0.21	0.04	2.94	3.2	0.3		9.3
300–310	305.0	0.93	3.79	68.7	1.46	2.04	0.36	0.05	4.09	2.8	0.3	1.4	8.9
310–320	315.0	0.96	3.25	71.2	1.36	2.00	0.32	0.05	3.80	2.9	0.3		8.8
320–330	325.0	2.49	7.98	57.7	2.47	2.74	0.66	0.08	5.59	1.5	0.0	1.2	–
330–340	335.0	0.54	3.16	69.4	1.37	1.99	0.32	0.05	3.78	3.0	0.4		8.2
340–350	345.0	0.94	4.07	67.7	1.53	2.09	0.38	0.06	4.36	2.3	0.3	1.6	8.1
350–360	355.0	0.84	4.80	65.2	1.72	2.16	0.45	0.06	4.65	1.7	0.0		–
360–362	361.0	–	–	–	–	–	–	–	–	–	–	–	–

Average

Stages	Depth	MgO	Al_2O_3	SiO_2	K_2O	CaO	TiO_2	MnO	Fe_2O_3	Carbon	Nitrogen	Sulfur	C/N
lacustrine	0–180 cm	1.25	4.43	35.7	1.83	2.43	0.45	0.09	8.99	14.8	1.3	3.9	11.3
marine	180–362 cm	0.79	4.29	66.2	1.55	2.18	0.38	0.07	4.17	2.8	0.3	1.5	8.7

Table 4. Concentrations of major elements (MgO, Al_2O_3, SiO_2, K_2O, CaO, TiO_2, MnO, and Fe_2O_3; average values of duplicate analyses), total carbon (TC), total nitrogen (TN), and total sulfur (TS) in core Ok5S recovered from L. Oyako.

Depth	Mid-depth	MgO	Al_2O_3	SiO_2	K_2O	CaO	TiO_2	MnO	Fe_2O_3	Carbon	Nitrogen	Sulfur	C/N
(cm)		(wt%)								(wt%)			
0–3	1.5	1.07	4.96	41.9	2.17	2.35	0.59	0.09	5.86	13.4	1.4	1.4	9.4
3–6	4.5	0.95	3.50	48.7	2.03	2.24	0.46	0.08	5.00	13.5	1.5	1.4	9.1
6–9	7.5	1.11	4.47	45.9	2.12	2.28	0.57	0.08	5.87	13.5	1.5	1.9	9.3
9–12	10.5	0.48	4.51	47.6	1.97	2.28	0.50	0.08	5.08	12.8	1.3	1.6	9.7
12–15	13.5	1.15	5.79	46.0	2.30	2.36	0.65	0.08	5.78	9.2	1.0	1.4	9.2
15–18	16.5	0.52	3.03	46.3	1.77	2.20	0.44	0.08	4.95	14.9	1.6	1.6	9.4
18–21	19.5	1.23	5.65	45.5	2.08	2.31	0.55	0.08	5.80	9.6	1.0	1.8	9.2
21–24	22.5	1.23	5.48	45.4	2.16	2.53	0.59	0.08	5.39	7.3	0.7	1.1	10.0
24–27	25.5	1.31	6.07	47.4	2.13	2.48	0.57	0.07	5.45	8.0	0.8	2.1	9.9
27–30	28.5	1.65	6.89	48.2	2.31	2.56	0.65	0.08	5.51	4.2	0.4	1.0	10.8
30–33	31.5	0.48	4.84	49.9	1.97	2.40	0.50	0.07	4.77	7.9	0.8	1.2	9.8
33–36	34.5	1.46	5.53	47.7	2.13	2.37	0.57	0.08	5.47	8.8	0.9	1.5	9.7
36–39	37.5	0.79	4.81	45.8	2.14	2.29	0.58	0.08	5.83	9.4	1.0	1.9	9.7
39–42	40.5	1.99	8.13	48.3	2.68	2.61	0.79	0.09	6.30	4.8	0.5	1.4	9.7
42–45	43.5	1.96	10.01	48.3	3.29	2.77	1.00	0.10	7.25	1.4	0.0	1.7	–
45–48	46.5	2.83	10.03	46.6	3.48	2.71	1.05	0.11	7.59	1.2	0.0	1.0	–
48–51	49.5	1.92	7.11	45.3	2.54	2.56	0.75	0.09	6.18	10.6	1.1	1.8	9.5
51–54	52.5	1.56	6.52	48.8	2.32	2.53	0.65	0.08	5.74	8.2	0.9	1.6	9.5
54–57	55.5	0.98	5.11	44.8	2.31	2.38	0.60	0.08	5.52	11.3	1.2	1.5	9.6
57–60	58.5	1.40	6.31	48.3	2.39	2.42	0.67	0.08	5.88	8.5	0.9	1.6	9.2
60–65	62.5	1.14	5.84	48.1	2.36	2.33	0.65	0.09	6.04	10.6	1.2	1.6	9.0
65–70	67.5	1.86	7.37	48.1	2.66	2.50	0.78	0.09	6.93	6.1	0.7	2.9	9.0
70–75	72.5	2.10	6.46	47.6	2.36	2.43	0.68	0.08	6.02	7.8	0.9	1.9	9.1
75–80	77.5	1.60	6.23	47.0	2.53	2.37	0.70	0.09	6.33	9.2	1.0	1.6	9.3
80–85	82.5	1.88	6.77	48.4	2.48	2.45	0.68	0.08	6.05	7.9	0.8	2.1	9.6
85–90	87.5	2.09	7.80	48.8	2.56	2.65	0.79	0.09	6.61	6.4	0.7	1.6	9.0
90–95	92.5	2.46	8.32	52.5	2.60	2.82	0.80	0.09	6.80	2.5	0.2	2.0	10.2
95–100	97.5	2.56	8.65	51.9	2.58	2.89	0.78	0.09	6.78	2.1	0.2	2.0	10.3
100–108	104.0	2.67	7.88	50.8	2.56	2.88	0.77	0.09	6.90	3.3	0.4	1.8	9.5
108–112	110.0	2.14	10.17	57.1	2.57	2.93	0.39	0.06	3.24	0.0	0.0	0.3	–
112–115	113.5	2.70	6.93	54.7	2.43	2.60	0.77	0.07	6.83	2.1	0.2	1.7	10.5
115–120	117.5	2.36	7.43	55.3	2.37	2.74	0.80	0.08	6.60	1.7	0.2	1.4	8.8
120–125	122.5	2.21	7.17	54.8	2.41	2.68	0.83	0.08	6.52	1.6	0.2	1.3	8.2
125–130	127.5	2.36	6.83	57.2	2.23	2.80	0.70	0.07	5.73	1.8	0.2	0.8	9.9
130–135	132.5	1.56	5.81	55.4	2.08	2.42	0.68	0.07	5.95	2.0	0.2	1.1	8.9
135–140	137.5	1.00	6.58	59.5	2.19	2.52	0.71	0.07	6.03	2.1	0.3	1.5	8.2
140–145	142.5	2.04	6.41	58.6	2.21	2.60	0.72	0.07	6.04	1.7	0.2	1.2	8.5
145–150	147.5	2.21	6.59	59.3	2.19	2.58	0.74	0.07	5.95	2.1	0.2	1.4	9.2
150–153	151.5	1.57	5.95	59.3	1.99	2.59	0.69	0.07	5.73	1.6	0.2	1.2	8.2

Average

Stages	Depth	MgO	Al_2O_3	SiO_2	K_2O	CaO	TiO_2	MnO	Fe_2O_3	Carbon	Nitrogen	Sulfur	C/N
lacustrine	0–90 cm	1.41	6.12	47.1	2.35	2.43	0.65	0.08	5.89	8.7	0.9	1.6	9.5
marine	90–153 cm	2.14	7.28	55.9	2.34	2.69	0.72	0.08	6.08	1.9	0.2	1.4	9.2

Table 5. Summary of fossil diatom data showing the relative abundance of freshwater and marine species in L. Skallen.

Depth (cm)	Mid-depth	Freshwater diatoms	Freshwater Chrysophyceae cysts	Marine diatom	Silicoflaggelates	Chaetoceros spores	Diatom stratigraphy	
							% Freshwater	% Marine
10–20	15	289	11	2	0	0	99.3	0.7
70–80	75	404	3	1	0	0	99.8	0.2
140–150	145	351	56	3	0	0	99.3	0.7
170–180	175	353	3	8	1	7	95.7	4.3
200–210	205	162	0	151	2	56	43.7	56.3
270–280	275	38	0	303	0	106	8.5	91.5
320–330	325	65	0	260	0	61	16.8	83.2

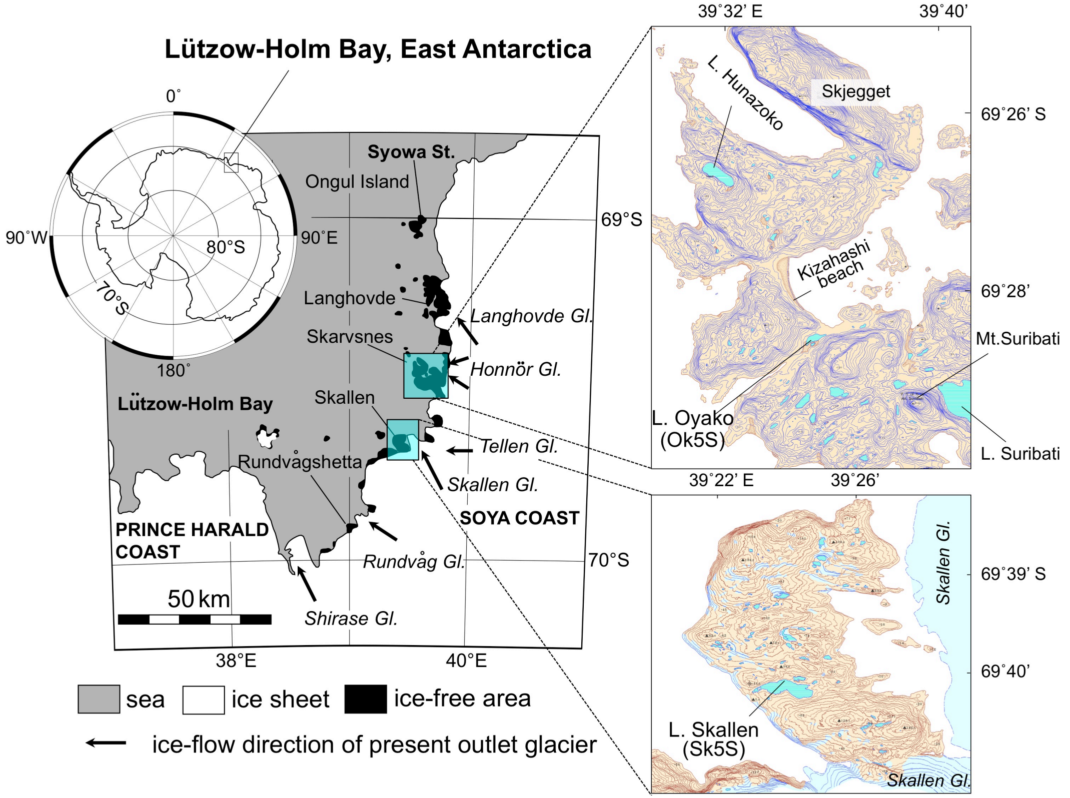

Fig. 1. Map showing the distribution of ice-free areas (Rundvågshetta, Skallen, Skarvsnes, and Langhovde) along the Soya Coast, East Antarctica. Arrows indicate the ice-flow directions of present-day outlet glaciers (see Sawagaki and Hirakawa, 1997). Also shown are detailed location maps of Lake Skallen Oike at Skallen and Lake Oyako at Skarvsnes. Topographic contours are based on compilation data from the Geographical Survey Institute (1973, 1987).

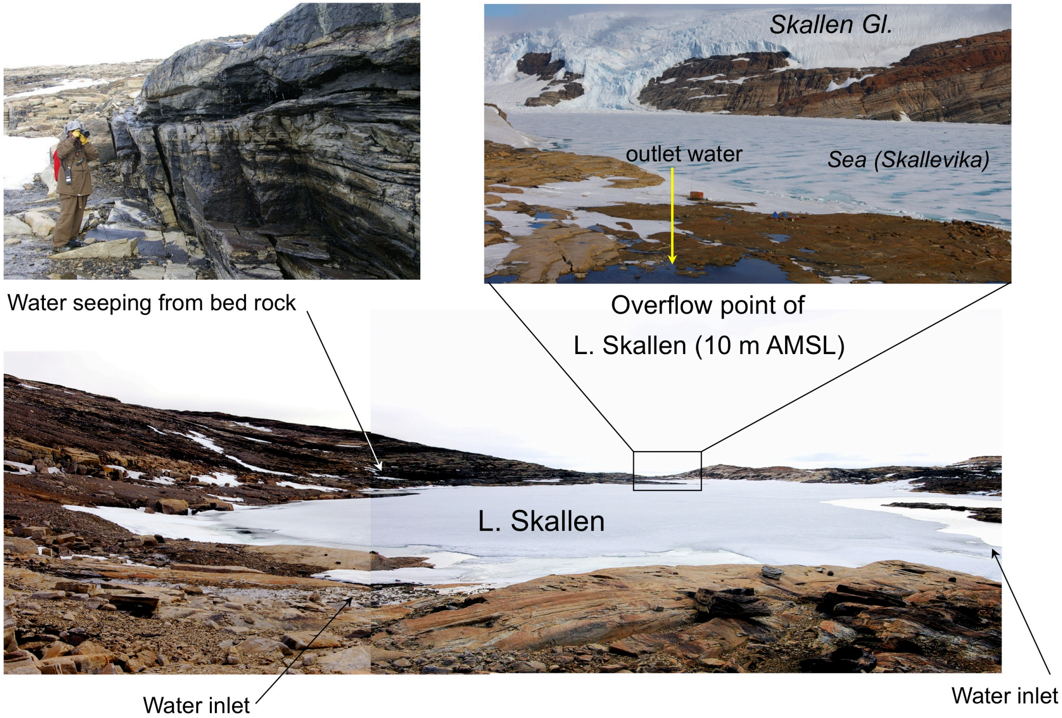

Fig. 2. Photographs of the landscape at L. Skallen, showing the water inlet and outlet (10 m a.m.s.l.), as taken in December 2005. The sediment core sample was collected from the lake center as shown in GPS data (Table 1). See also the landscape and freshwater biota in L. Oyako (Tanabe et al., 2008).

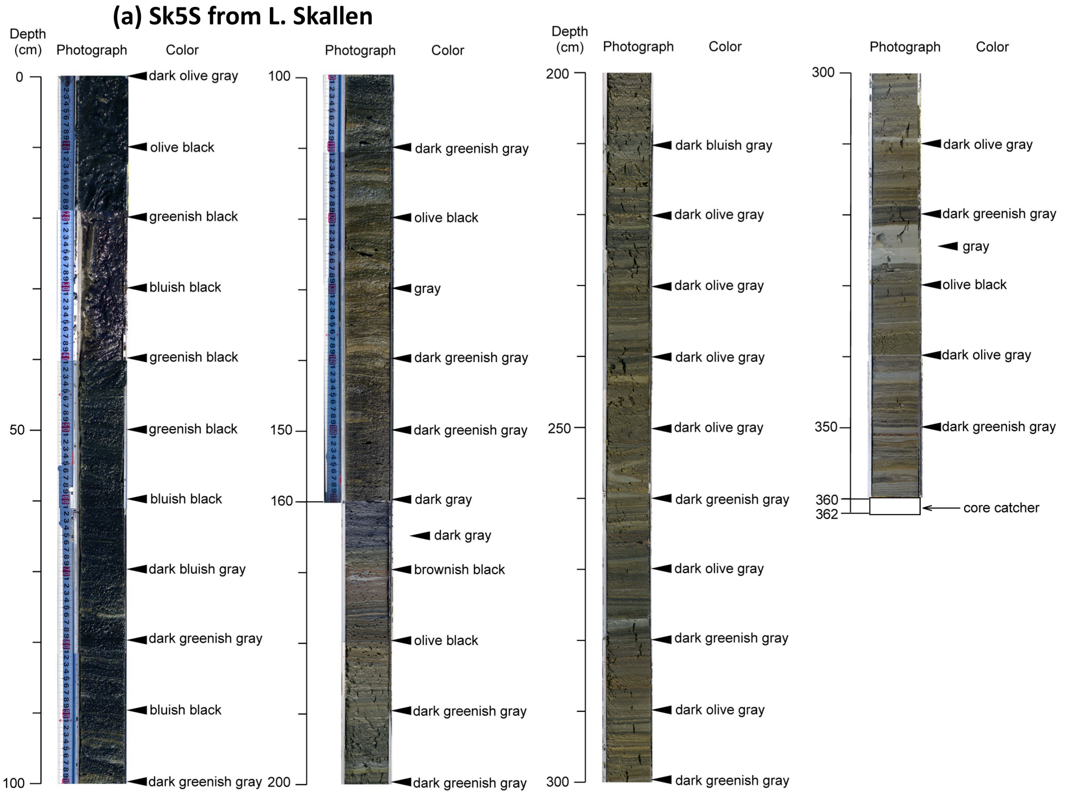

Fig. 3. (a) Photographs of the sediment core Sk5S obtained from L. Skallen.

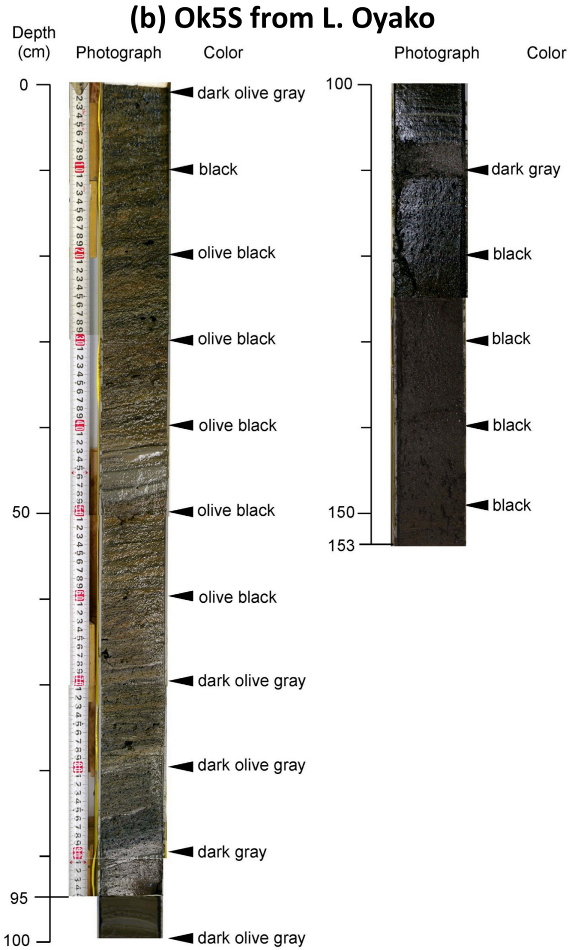

Fig. 3. (b) Photographs of core Ok5S obtained from L. Oyako. The color data was expressed by Standard Soil Color Charts.

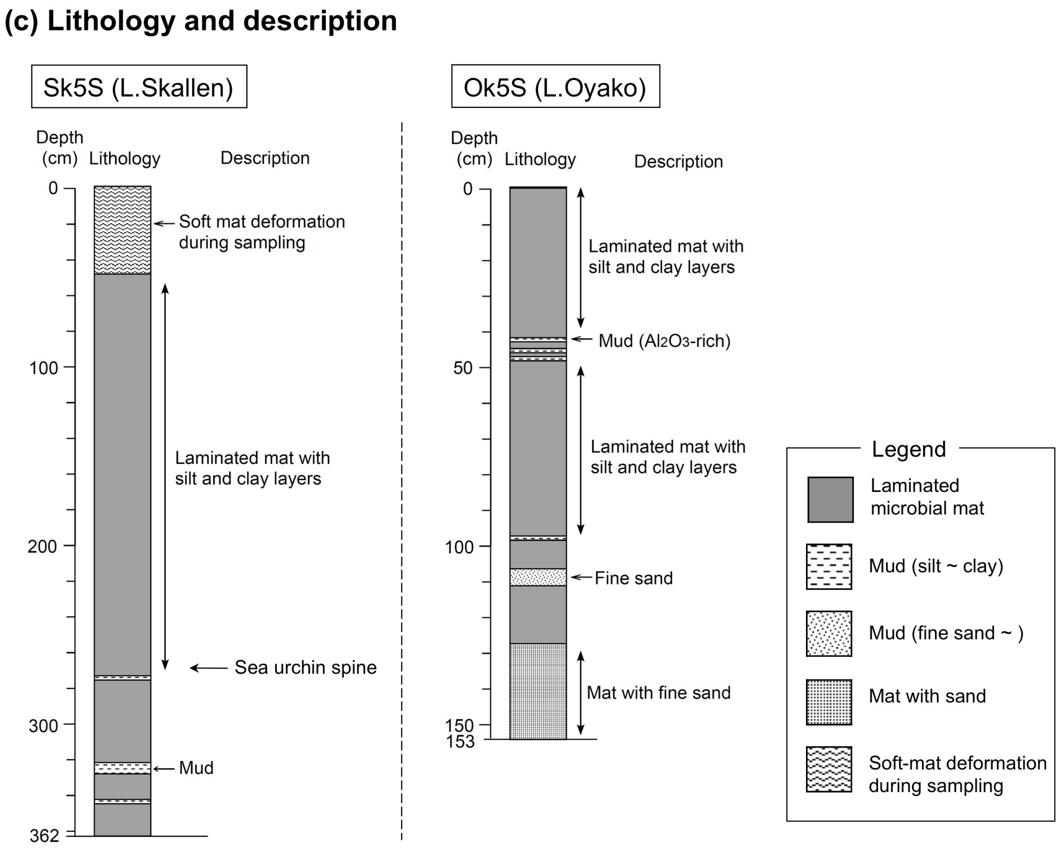

Fig. 3. (c) Lithology and description of cores Sk5S and Ok5S.

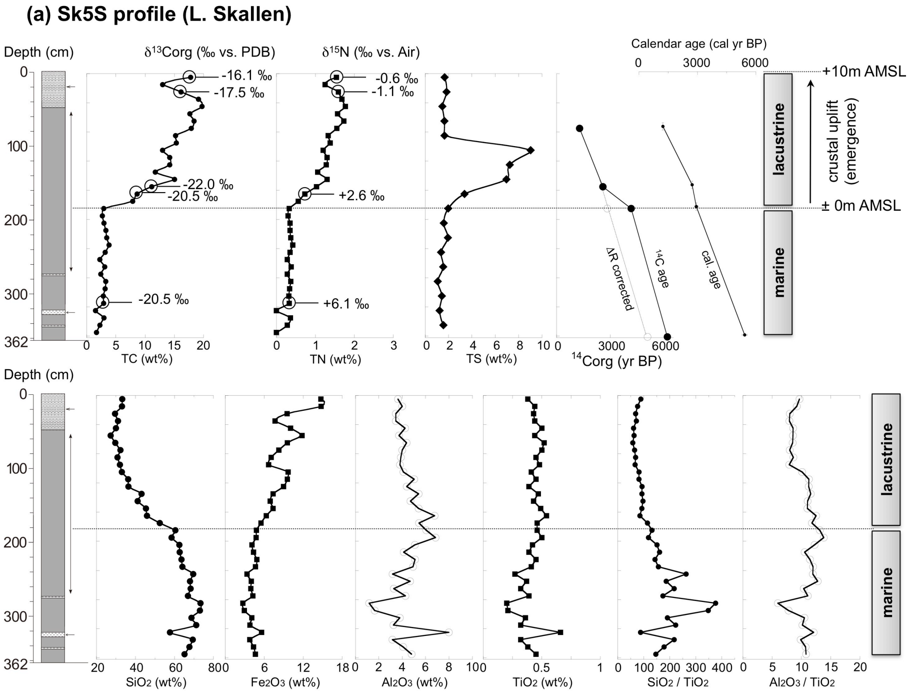

Fig. 4. Sedimentary facies defined by total carbon (TC), total nitrogen (TN), total sulfur (TS), and age data for cores Sk5S **(a)** and Ok5S **(b)**. $\delta^{13}C_{org}$ (‰ vs. PDB) and $\delta^{15}N$ (‰ vs. air) data (following HCl treatment to collect the organic fraction) are shown with the circled sequential depth. Conventional radiocarbon dating of sedimentary organic carbon ($^{14}C_{org}$, yr BP) and correction for the marine reservoir effect (ΔR_{org} as 1100 yr) are based on previous studies (Yoshida and Moriwaki, 1979; Hayashi and Yoshida, 1994; Ingolfsson et al., 1998). Calendar age data were calculated using the calibration program Calib Rev 5.0.1 (Stuiver et al., 1993, 1998) for INTCAL and MARINE (Hughen et al., 2004; Reimer et al., 2004). Major element concentrations (dry, wt%) for SiO_2, Fe_2O_3, Al_2O_3, and TiO_2 are shown for L. Skallen and L. Oyako (Tables 3 and 4).

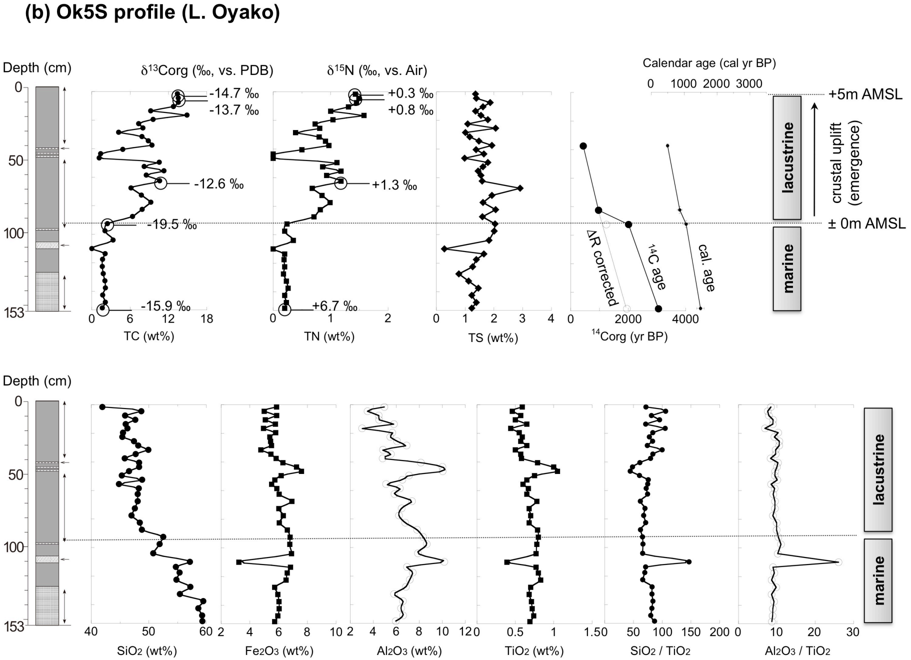

Fig. 4. Continued.

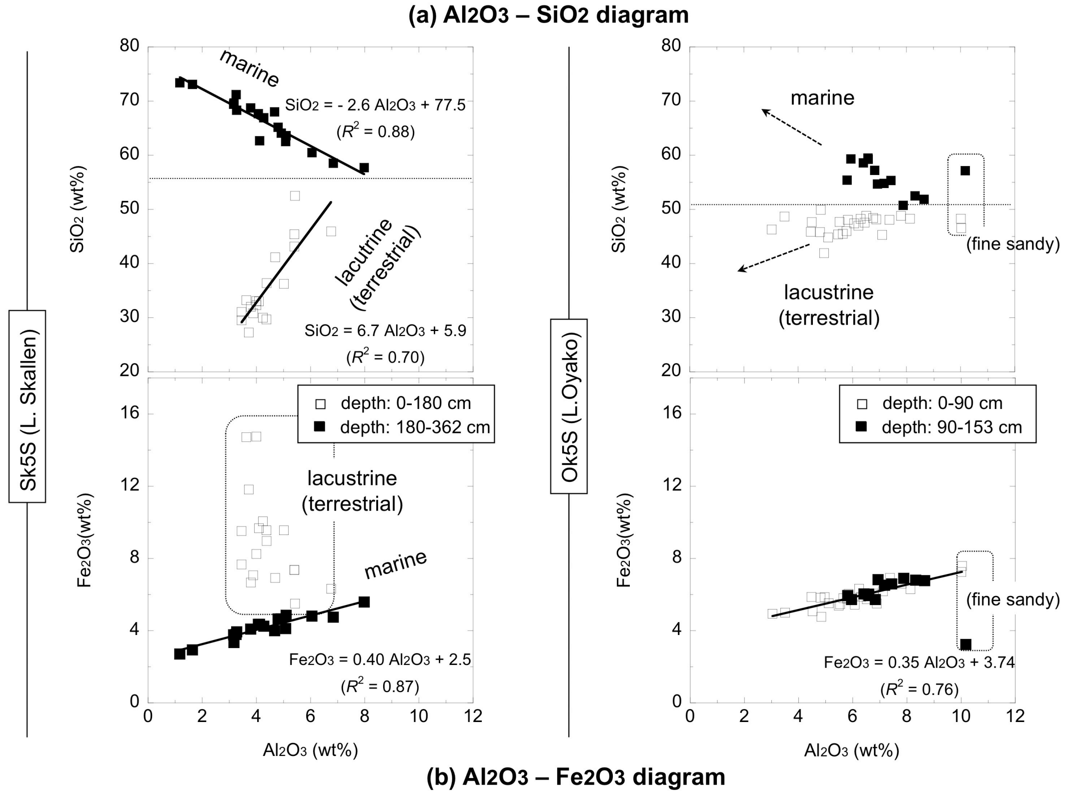
(a) Al2O3 – SiO2 diagram

(b) Al2O3 – Fe2O3 diagram

Fig. 5. (a) Diagram of Al_2O_3 (wt%) vs. SiO_2 (wt%) and the end-member profiles from Sk5S and Ok5S cores, divided into marine and lacustrine sedimentary stages (see Fig. 4). Possible surge events represented by fine sandy layers are also plotted for Ok5S. **(b)** Diagram of Al_2O_3 (wt%) vs. Fe_2O_3 (wt%) and the end-member profiles from Sk5S and Ok5S cores, divided into marine and lacustrine sedimentary stages (see Fig. 4).

Title Page
Abstract
Introduction
Conclusions
References
Tables
Figures
◀▮
▶▮
◀
▶
Back
Close
Full Screen / Esc
Printer-friendly Version
Interactive Discussion

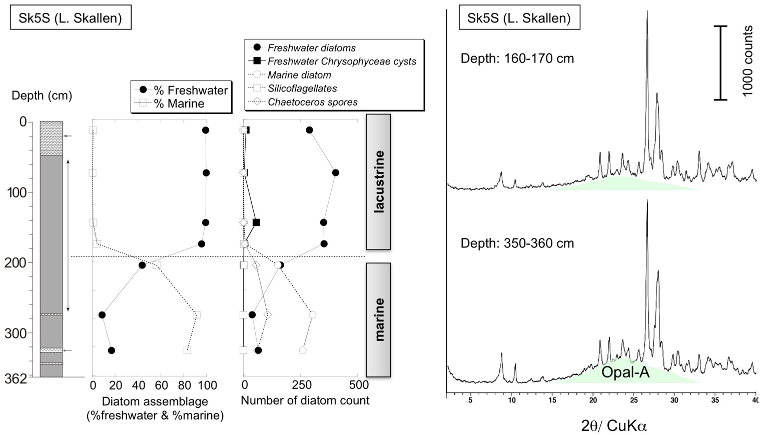
(a) Biological facies of fossil diatom

(b) Opal-A identified by XRD

(c) Facies fossil

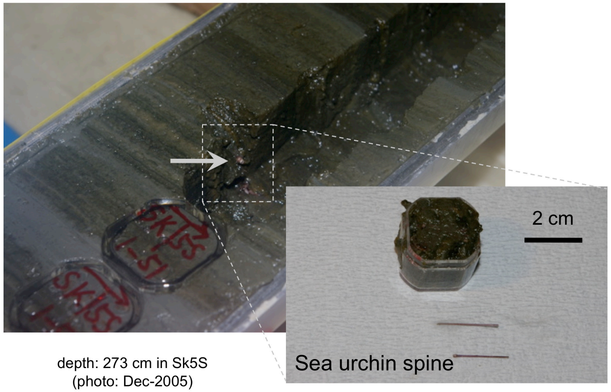

Fig. 6. **(a)** Biological facies of fossil diatoms, showing the relative abundance of freshwater and marine species (Table 5). **(b)** Representative 2 θ peaks of Opal-A, as obtained by X-ray diffraction (XRD) analysis (Mac Science Co. Ltd.), for sample from core Sk5S. **(c)** We found a fossil of sea urchin spine at the depth of 273 cm (paleo-magnetism sample section) in L. Skallen sediment.

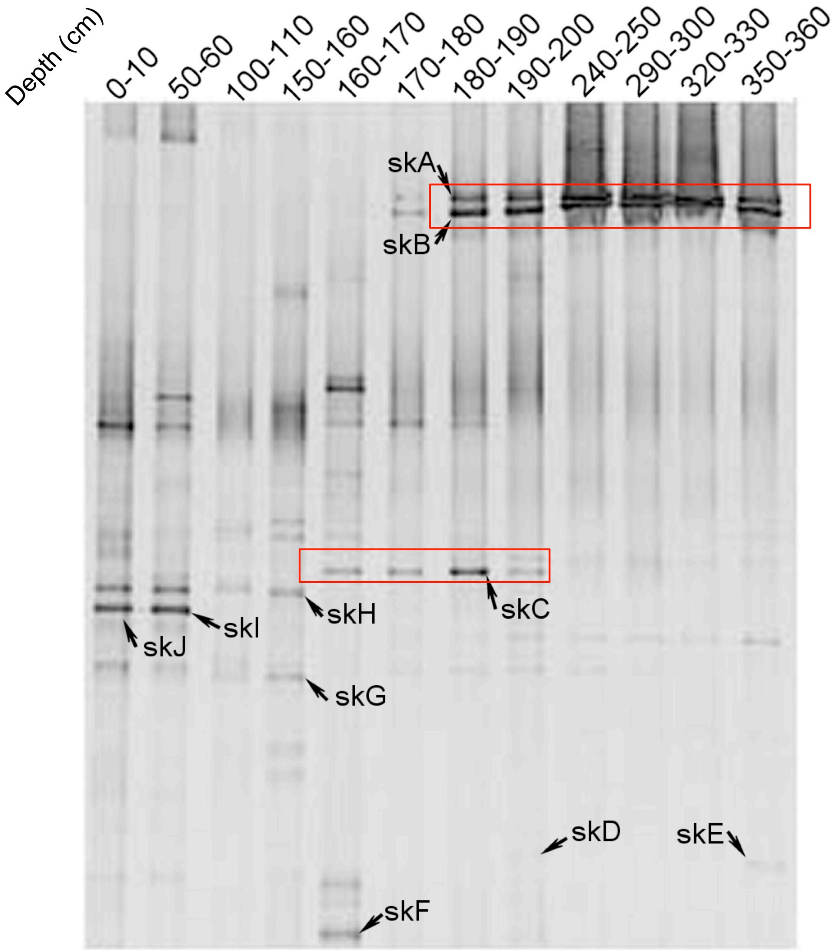

Fig. 7. DGGE band patterns of the 16S rRNA gene fragments. Numbers on the lanes indicate sediment depths (cm).

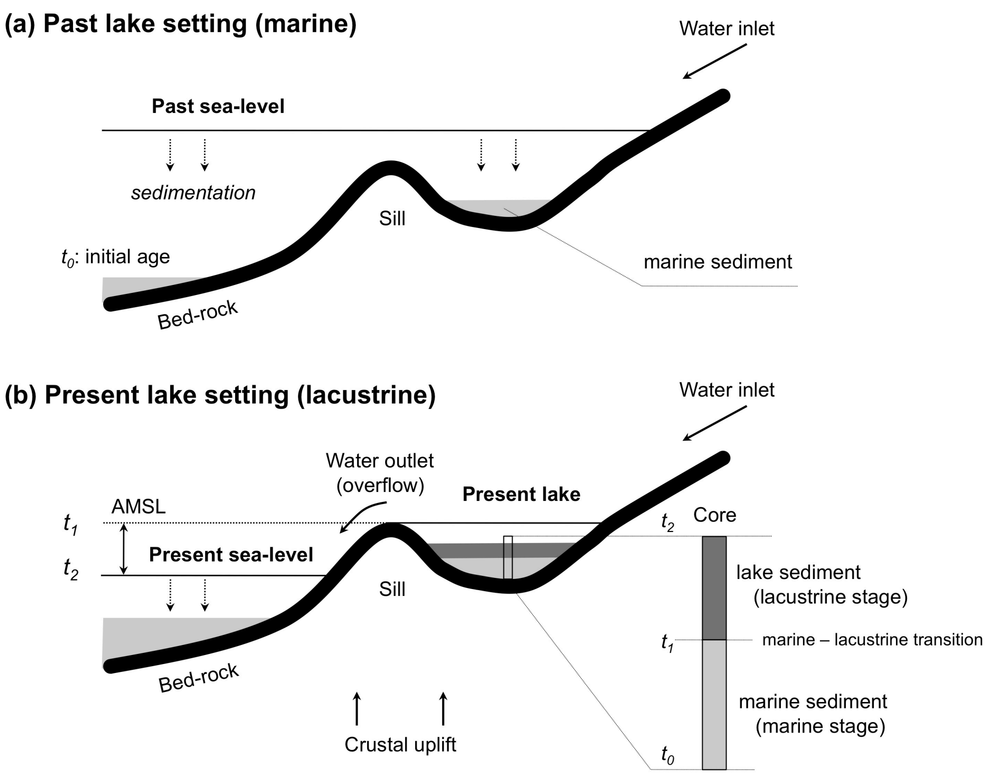

Fig. 8. Schematic representation of the uplift-related emergence event that marked the transition between marine and lacustrine sedimentary stages. **(a)** Past lake setting; the time t_0 represents the timing of the initial deposition of sediment upon bedrock following the cessation of glacial erosion. **(b)** Present lake setting; the times t_1 and t_2 represent the emergence age (transition from marine to freshwater including temporal brackish condition; a.m.s.l.$_{t=1}$) and the present age (a.m.s.l.$_{t=2}$), respectively. Precisely, the record of relative sea-level changes could be estimated from present sill height and sea-level (a.m.s.l.).

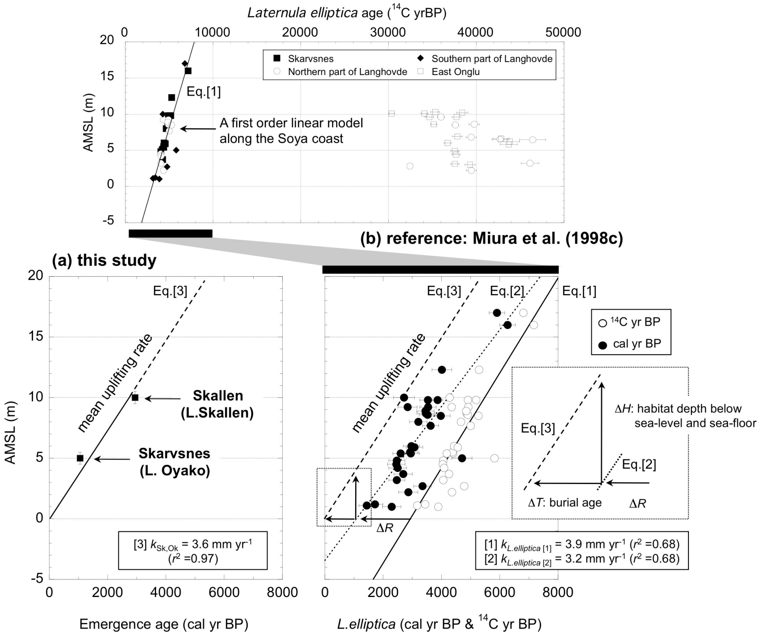

Fig. 9. (a) Linear approximation model of emergence age (cal yr BP, Eq. 3) based on the transition from marine to lacustrine sedimentary facies in the obtained cores. Here, the correlation coefficient (r^2=0.97) is shown as a linear extrapolation plot. Tidal ranges represented in the error bars of a.m.s.l. data were taken from sea-level observations performed along the Soya Coast, Lützow-Holm Bay (Aoki et al., 2000). **(b)** Linear approximation model of reference data compiled from raw data for *L. elliptica* fossils from the Soya coast along Lützow-Holm Bay (Miura et al., 1998c). White circles (^{14}C yr BP) represent radiocarbon data (Eq. 1 for the proposed rate constant $k_{L.\ elliptica\,[1]}$; raw data from Miura et al., 1998c) fitted by a linear approximation model. Black circles (cal yr BP) represent the proposed rate constant $k_{L.\ elliptica[2]}$ from calculated using Eq. (1), taking into account the marine reservoir effect and calibrated using Calib Rev 5.0.1. ΔH represents the sum of the habitat depth below sea-level plus that below the sea floor during the lifecycle of *L. elliptica* (see also Fig. 10) with latter re-deposition thickness of sediment. Here, a marine reservoir correction ($\Delta R_{L.\ elliptica}$) for the reference data was tentatively based on a calcareous marine fossil correction of 1,300±100 years (Berkman et al., 1996). All of the data shown here are presented in the map of Miura et al. (1998c) and references therein.

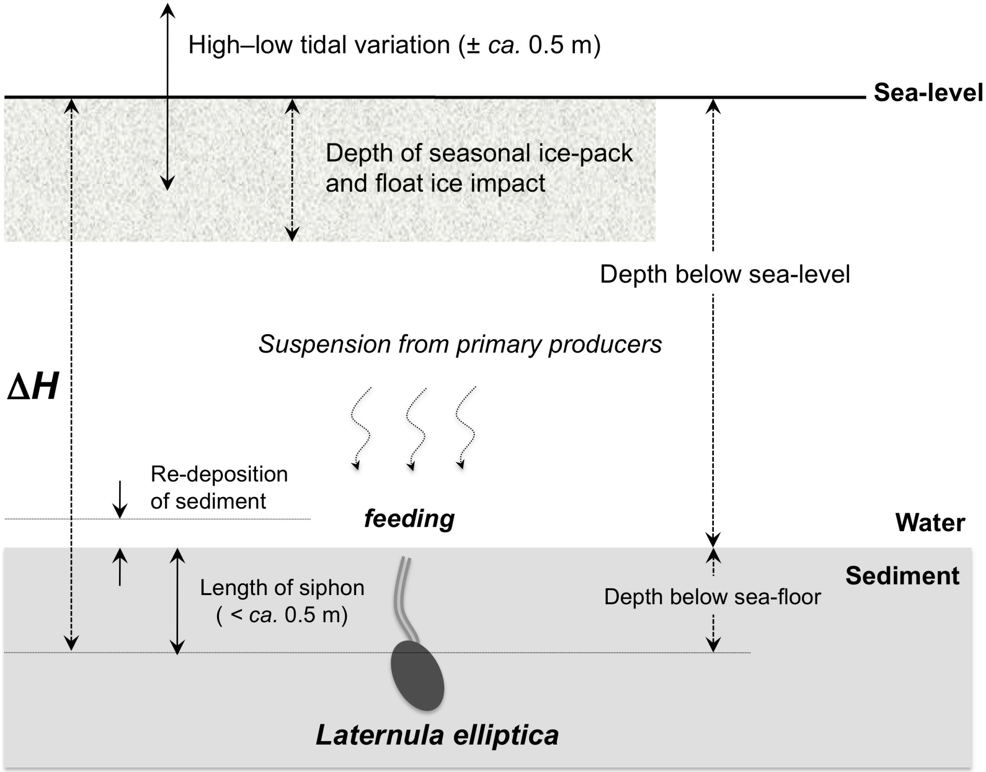

Fig. 10. Proposed interpretation of the offset among the sea-level record from the bivalve suspension feeder *Laternula elliptica*. Water depth in the subtidal environment can be estimated as the difference Δ*H*: habitat depth below sea-level plus that below the sea floor during the lifecycle of *L. elliptica*. The secondary re-deposition process has to be also considered within Δ*H* distance. Based on an ecological description of the living environment of *L. elliptica*, the length of the siphon corresponds to depth below the sea floor. Tidal range (within ±0.5 m) within Lützow-Holm Bay, East Antarctica, is based on existing data (e.g. Aoki et al., 2000).

Title Page
Abstract | Introduction
Conclusions | References
Tables | Figures
◀| |▶
◀ ▶
Back | Close
Full Screen / Esc
Printer-friendly Version
Interactive Discussion

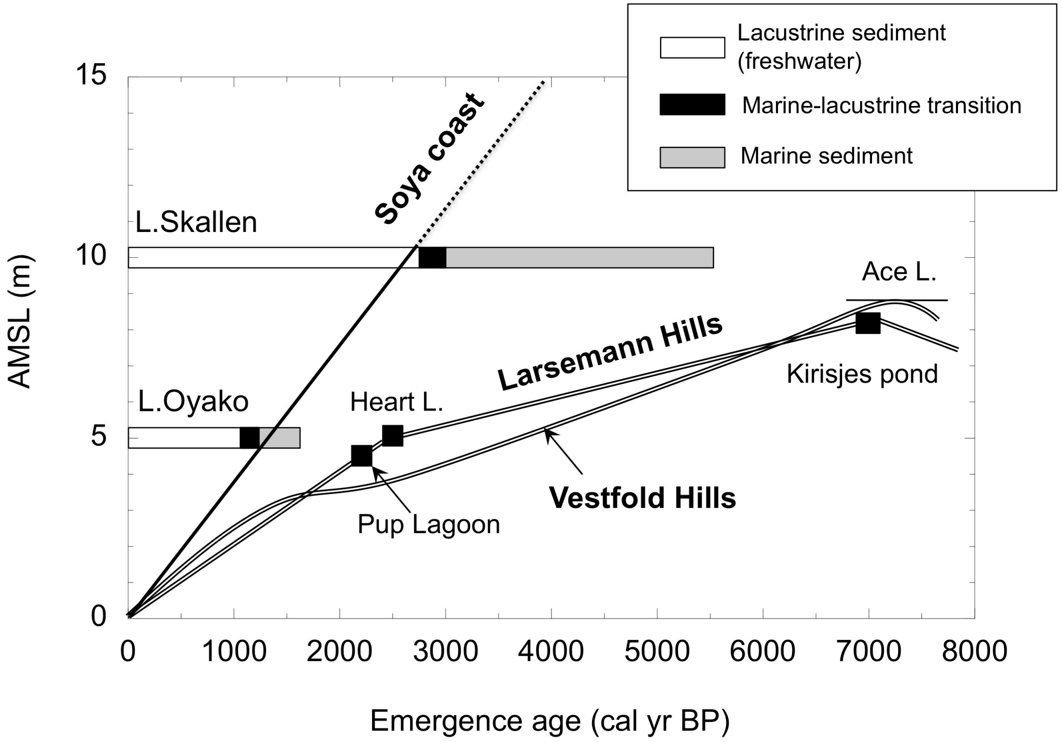

Fig. 11. Comparison of relative sea-level changes in the Soya coast along Lützow-Holm Bay (this study: single solid line and dashed line), Larsemann Hills (double line), and Vestfold Hills (double line). The Larsemann Hills curve was based on the sediment sequences from Kirisjes Pond, Heart Lake, and Pup Lagoon (Verleyen et al., 2005). The marine-lacustrine transitions of those three lakes were plotted. The Vestfold Hills curve was based on sediment sequences from Ace lake, Anderson lake, Highway lake, Watts lake, and Organic lake (Roberts and McMinn, 1999; Zwartz et al., 1998). The Holocene marine-limit of Ace lake was noted.